

QCD SUM RULES FOR THE ANTICHARMED PENTAQUARK

A THESIS SUBMITTED TO
THE GRADUATE SCHOOL OF NATURAL AND APPLIED SCIENCES
OF
MIDDLE EAST TECHNICAL UNIVERSITY

BY

YASEMİN SARAÇ

IN PARTIAL FULFILLMENT OF THE REQUIREMENTS
FOR
THE DEGREE OF DOCTOR OF PHILOSOPHY
IN
PHYSICS

JANUARY 2007

Approval of the Graduate School of Natural and Applied Sciences.

Prof. Dr. Canan Özgen
Director

I certify that this thesis satisfies all the requirements as a thesis for the degree of Doctor of Philosophy.

Prof. Dr. Sinan Bilikmen
Head of Department

This is to certify that we have read this thesis and that in our opinion it is fully adequate, in scope and quality, as a thesis for the degree of Doctor of Philosophy.

Prof. Dr. Ahmet Gökalp
Supervisor

Examining Committee Members

Prof. Dr. Mehmet Abak (Hacettepe Univ., PHED)_____

Prof. Dr. Ahmet Gökalp(METU, PHYS) _____

Prof. Dr. Osman Yılmaz(METU, PHYS) _____

Prof. Dr. Ersan Akyıldız(METU, MATH) _____

Assoc. Prof. Dr. Altuğ Özpıneci (METU, PHYS)_____

“I hereby declare that all information in this document has been obtained and presented in accordance with academic rules and ethical conduct. I also declare that, as required by these rules and conduct, I have fully cited and referenced all material and results that are not original to this work.”

Name, Last name : YASEMİN SARAÇ

Signature :

ABSTRACT

QCD SUM RULES FOR THE ANTICHARMED PENTAQUARK

Saraç, Yasemin

Ph.D., Department of Physics

Supervisor: Prof. Dr. Ahmet Gökcalp

January 2007, 83 pages.

For the anti-charmed pentaquark state with and without strangeness a QCD sum rule analysis, which is one of the nonperturbative approaches, is presented. For this purpose we employ pentaquark currents with and without strangeness, with two different current for each case. To refine the sum rules we also consider the DN continuum contribution in our analysis since this procedure is important to identify the signal of the pentaquark state. While the sum rules for most of the currents are either non-convergent or dominated by the DN continuum, the one for the non-strange pentaquark current composed of two diquarks and an antiquark, is convergent and has a structure consistent with a positive parity pentaquark state after subtracting out the DN continuum contribution. Arguments are presented on the similarity between the result of the present analysis

and that based on the constituent quark models, which predict more stable pentaquark states when the antiquark is heavy.

Keywords: Charmed pentaquark, QCD sum rules, DN continuum, Exotic hadrons.

ÖZ

ANTI-CAZİBELİ PENTAKUARK İÇİN KUANTUM RENK DİNAMİĞİ TOPLAMA KURALLARI

Saraç, Yasemin

Doktora, Fizik Bölümü

Tez Yöneticisi: Prof. Dr. Ahmet Gökarp

Ocak 2007, 83 sayfa.

Acayip kuark içeren ve içermeyen anti-cazibeli pentakuark durumu için perturbatif (tedirgemesi) olmayan yaklaşımlardan biri olan kuantum renk dinamiği toplama kuralları analizi yapıldı. Bu amaçla acayip kuark içeren ve içermeyen her pentakuark akımı için iki ayrı akım kullanıldı. Pentakuark durumundan gelen sinyali belirlemekte önemli olması nedeniyle analize toplama kurallarını iyileştirmek için DN sürekliliği de katıldı. Toplama kuralı akımların çoğu için ıraksak ya da DN sürekliliğinin baskın olmasına karşın acayip kuark içermeyen ve iki ikili-kuark ve bir antikuark içeren pentakuark akımı için olan toplama kuralı yakınsaktır ve DN sürekliliği çıkartıldıktan sonra pozitif pariteli pentakuark durumuna uygun bir yapıya sahiptir. Buradaki analizler ile antikuark ağır olduğunda daha kararlı bir pentakuark tahmini veren kuark modeline dayanan

analizler arasındaki benzerlikler üzerine argümanlar sunulmuştur .

Anahtar Kelimeler: Cazibeli pentakuark, Kuantum Renk Dinamiği toplama kuralları, DN sürekliliği, Egzotik hadronlar.

...ANNEME

VE

BABAMA...

ACKNOWLEDGMENTS

I am extremely grateful to three people for their unlimited help and support to complete this thesis.

First of all I would like to express my deepest gratitude to my advisor Prof. Dr. Ahmet Gökalp. Without his excellent supervision, encouragement, invaluable comments and helps, patience, continuous support and careful reading I would never have been able to undertake and carry out this work.

Nor can I forget what I owe to Prof. Dr. Osman Yılmaz who has made countless productive and useful suggestion in every part of this work, which has greatly benefited from his careful reading and critical comments. I would like to especially thank him once again because of his friendly attitude, patience, supervision and for giving me such a great opportunity to work with him.

I am also deeply indebted to Prof. Dr. Su Hounq Lee who thought me the QCD sum rules and offered me the subject of this thesis. His advice, supervision and crucial contribution made him a backbone of this research and so to this thesis. I am grateful in every possible way and hope to keep up our collaboration in the future.

This thesis owe very much to Altuğ Özpineci who took the time to iron out

many mistakes. He provided very helpful feedback and always answered my questions no matter how odd.

I am also thankful to Assoc. Prof. Dr. Hungchong Kim for the invaluable help during my learning the subject of QCD sum rules.

Many great thanks are also due to my family; my mom, my dad , my sister Esin and my brother Yasin for their continuous support, encouragement and understanding.

And special thanks to my husband Hüseyin for his endless love, faith and understanding.

Finally I am particularly indebted to all my friends for their support.

TABLE OF CONTENTS

ABSTRACT	iv
ÖZ	vi
DEDICATION	viii
ACKNOWLEDGMENTS	viii
TABLE OF CONTENTS	xi
LIST OF FIGURES	xiii
CHAPTER	
1. INTRODUCTION	1
2. QCD SUM RULES	8
2.1 QCD Sum Rules	8
2.2 Phenomenological Representation and Dispersion Relation	11
2.3 Operator Product Expansion	14
2.4 Analytic Continuation	16
2.5 Borel Transform And Sum Rules	17
2.6 Vacuum Condensates	21
3. QCD SUM RULES FOR ANTICHARMED PENTAQUARK Θ_c .	26
3.1 Interpolating Field for Θ_c	26
3.2 Dispersion Relation	28
3.3 Phenomenological Side	31

3.3.1	Θ_{c1} and Θ_{cs1}	31
3.3.2	Θ_{c2} and Θ_{cs2}	34
3.3.3	Final Form of the Phenomenological Side	35
3.4	OPE Side	36
3.4.1	The OPE for Θ_{c1}	36
3.4.2	The OPE for Θ_{c2}	45
3.4.3	The OPE for Θ_{cs1}	47
3.4.4	The OPE for Θ_{cs2}	51
4.	QCD SUM RULES AND ANALYSIS	54
4.1	The Couplings to the DN Continuum, λ_{DN}	54
4.2	Parity	56
4.3	Mass	59
5.	CONCLUSIONS	62
	REFERENCES	64
	APPENDICES	69
A.	NOTATIONS	69
B.	GAMMA MATRIX ALGEBRA	71
C.	TRACES AND CONTRACTIONS	74
D.	USEFUL INTEGRALS AND EQUATIONS	76
E.	THE FULL PROPAGATOR FOR THE LIGHT QUARK	78
F.	THE BOREL TRANSFORMATION	79

LIST OF FIGURES

FIGURES

- Figure 2.1 The contour in the plane of the complex variable $q^2 = z$. The open point indicates the $q^2 < 0$ reference point of the QCD calculations and the crosses indicates the positions of hadronic thresholds at $q^2 > 0$ 18
- Figure 3.1 Schematic OPE diagrams for the current Θ_{c1} in Eq. (3.2). Each label corresponds to that in Eq. (3.41). The solid lines denote quark (or anti-charm quark) propagators and the dashed lines are for gluon. The crosses denote the quark condensate, and the crosses with circle represent the mixed quark gluon condensates. (c) represents diagrams proportional to gluon condensate with gluons lines attached to the light quarks only, (d) represents those where the gluons are attached to the heavy quarks only, while (e) represents those where one gluon is attached to the heavy quark and the other to a light quark in all possible ways. (f) and (g) represent all diagrams that contain the quark-gluon condensate. 37
- Figure 3.2 OPE as defined in Eq. (3.42) for the current Θ_{c1} and $S_0 = (3.3 \text{ GeV})^2$. The left (right) figure is for positive (negative) parity case. The solid line (a) represents the perturbative contribution. The line specified as OPE represents the sum of the power corrections only. (c) represents the gluon condensates. Other labels represent contribution from each term in Eq. (3.41). Here we plot only a few selected terms in the OPE. 44
- Figure 3.3 Schematic OPE diagrams for the current Θ_{c2} in Eq. (3.44). Each label corresponds to that in Eq. (3.44). All the other notations in this figure are the same as Fig. 3.1. 46
- Figure 3.4 A similar figure as Fig. 3.2 for the current Θ_{c2} . Here each label represents contribution from each term in Eq. (3.44). The gluon condensates (b) are the dominant power correction in the positive parity channel (left figure). 48

Figure 3.5	Schematic OPE diagrams for the currents Θ_{cs1} in Eq. (3.45) and Θ_{cs2} in Eq. (3.46). Each label corresponds to that in Eq. (3.45) or Eq. (3.46). All the other notations in this figure are the same as Fig. 3.1.	49
Figure 3.6	A similar figure as Fig. 3.2 for the current Θ_{cs1} with $S_0 = (3.3 \text{ GeV})^2$. Here each label represents contribution from each term in Eq. (3.45).	51
Figure 3.7	A similar figure as Fig. 3.2 for the current Θ_{cs2} with $S_0 = (3.3 \text{ GeV})^2$. Here each label represents each term in Eq. 3.46 . . .	53
Figure 4.1	The $ \lambda_{DN,c2} ^2$ from the sum rule for $i = q$ (solid) line and $i = 1$ (dashed line). The upper (lower) solid or dashed lines in this case are for $S_0 = (3.8 \text{ GeV})^2$ [$S_0 = (3.7 \text{ GeV})^2$].	55
Figure 4.2	The left figure shows the left-hand side of Eq. (4.3) using Θ_{c2} for positive parity case with $ \lambda_{DN,c2} ^2 = 2 \times 10^{-5} \text{ GeV}^{10}$ (dashed line) and $ \lambda_{DN,c2} ^2 = 3 \times 10^{-5} \text{ GeV}^{10}$ (dot-dashed line). The solid line is when there is no DN continuum, $ \lambda_{DN,c2} ^2 = 0$. The right figure is obtained with different threshold parameters. See Eq. (3.12) for A and B	57
Figure 4.3	The left figure shows the left-hand side of Eq. (4.3) using Θ_{c2} for negative parity case with $ \lambda_{DN,c2} ^2 = 2 \times 10^{-5} \text{ GeV}^{10}$ (dashed line) and $ \lambda_{DN,c2} ^2 = 3 \times 10^{-5} \text{ GeV}^{10}$ (dot-dashed line). The solid line is when there is no DN continuum. The right figure is obtained with different threshold parameters.	58
Figure 4.4	The mass obtained by taking the square root of the inverse ratio between left hand side of Eq. (4.3) and its derivative with respect to M^2 using Θ_{c2}	60

CHAPTER 1

INTRODUCTION

The observation of the pentaquark state Θ^+ by the LEPs collaboration [1] and its subsequent confirmation have brought a lot of excitement in the field of hadronic physics [2]. On the other hand, there are increasing number of experiments reporting negative results. In particular, the latest experiments at JLAB [3] find no signal from the photoproduction process on a deuteron nor on a proton target, from which the Θ^+ was observed earlier by the SAPHIR collaboration with lower statistics. Although the present experimental results are quite confusing and frustrating [4], one can not afford to give up further refined experimental search, because if a pentaquark is found, it will provide a major and unique testing ground for quantum chromo dynamics (QCD) dynamics at low energy.

Other multiplet to search for a possible pentaquark states are those with one heavy antiquark. The H1 collaboration at HERA has recently reported on the finding of an anti-charmed pentaquark $\Theta_c(3099)$ from the D^*p invariant mass spectrum [5]. Unfortunately other experiments could not confirm the finding [6,

7, 8]. While the experimental search for the heavy pentaquark is as confusing as that for the light pentaquark, theoretically, the heavy and light pentaquarks stand on quite different grounds. Cohen showed that the original prediction for the mass of the Θ^+ based on the SU(3) Skyrme model, which resulted in a mass value 1530 MeV [9], is not valid because collective quantization of the model for the anti-decuplet states is inconsistent in the large N_c limit [10]. In contrast, many theories consistently predicted a stable heavy pentaquark state. The pentaquark with one heavy anti-quark was first studied in Ref. [11, 12] in a quark model with color spin interaction. In Ref. [11] it was stated that the pentaquark states with the quark contents P^0 ($\bar{c}uuds$) and P^- ($\bar{c}ddus$) with spin- $\frac{1}{2}$ and their beauty analogs have very good chances to become stable, but with a refined analysis they turned out to be unstable [13]. Then it has been studied in quark models with flavor spin interaction [14, 15] and in Ref. [14] it was pointed out that the non-strange positive parity pentaquarks are the best candidates for stable compact systems in contrast to the negative parity pentaquarks studied in Ref. [15] in which it was suggested that pentaquarks of negative parity are unstable. In addition to this there are important similarities between the result of Ref. [14] and Ref. [16] which stated that the lowest pentaquark states have positive parity for any flavor content and it is not necessary to contain strangeness to become stable. In Ref. [14] the mass value for positive parity non-strange pentaquark was obtained as $m(uudd\bar{c}) = 2.895$ GeV. Another study was made using Skyrme

models [16, 17] and in Ref. [16] it was predicted that both the strange and non-strange pentaquarks might be stable. And Oh et al. [17] also stated a possibility for the loosely bound non-strange pentaquark baryons. Although the binding energy and the mass formula they used were different from the ones of Riska and Scoccola [16] their results supported the result of [16]. Skyrme model calculation was also applied in Ref. [18, 19, 20] for the pentaquark baryons whose result showed a possibility of stable pentaquarks. And with the recent experiments, pentaquarks have attracted renewed interests [21, 22, 23, 24, 25, 26, 27, 28, 29]. Cheung [21] employed the color-spin hyperfine interaction by considering the picture of diquark-diquark-antiquark [30] and diquark-triquark [31] and obtained that the diquark-diquark-antiquark picture gives the most favorable hyperfine interaction while the diquark-triquark picture gives a slightly higher hyperfine interaction. Cheung also obtained the mass of the Θ_c between 2938 and 2997 MeV. In Ref. [23] Nowak et al. discussed the possibility to interpret the mass of the charmed pentaquark state in the chiral doubler scenario, forcing each heavy light hadron to have opposite parity partner. In Ref. [28] using the quark model with spin color interaction properties of the mass spectrum of the exotic states was derived in an expansion in $\frac{1}{N_c}$. A mass estimation for exotic state and the discussion about their weak decay were made in Ref. [29] considering the possible existence of the pentaquark state, with a heavy antiquark, \bar{b} or \bar{c} and two light diquarks in a relative S-wave, which are stable against strong decay. Pentaquark

states are also studied in a coupled channel approach [32], and in the combined large N_c and heavy quark limit of QCD [33]. If the heavy pentaquark state is stable against strong decay, as was predicted in the D meson bound soliton models [16], it could only be observed from the weak decay of the virtual D meson. From a constituent quark model picture based on the color spin interaction [34], one expects a strong diquark correlation, from which one could have a stable diquark-diquark-antiquark [30] or diquark triquark [12] structure. The question is whether such strong diquark structure will survive other non-perturbative QCD dynamics in a multiquark environment and produce a stable pentaquark state. Such questions are being intensively pursued in quark model approaches [35, 38, 39]. Hiyama et al. [35] obtained no resonance in reported energy region of $\Theta^+(1540)$ by solving the five-quark scattering problem by applying Gaussian expansion method [36] and the Kohn-type variational method [37] to the large model space including the KN (Kaon-Nucleon) scattering component. In Ref. [39] the result of fully-antisymmetrized Goldstone boson and color magnetic model calculations for the hyperfine energies of heavy pentaquark states was presented and the mass value $m_{\Theta_c} \simeq 2835 \pm 30$ MeV, which puts the Θ_c just above the corresponding strong decay threshold, was obtained. In particular, an important question at hand is whether the net attraction from the diquark correlations in the pentaquark configuration is stronger than that coming from the corresponding diquark and additional quark-antiquark correlation present when the pentaquark

separates into a nucleon and a meson state. Since the correlation is inversely proportional to the constituent quark masses involved, the attraction is expected to be more effective for pentaquark state with heavy antiquark. Another non-perturbative approach that can be used to answer such question is the QCD sum rules method.

There have been several QCD sum rules calculations for the light pentaquark states [40, 41, 42, 43, 44, 45, 46, 47]. Zhu [40] employed QCD sum rules to estimate the mass of the pentaquark state with $J = \frac{1}{2}$ and $I = 0, 1, 2$. Matheus et al. [41] explored the diquark-diquark-antiquark state proposed by Jaffe and Wilczek [30] as a possible organization of the quarks in $\Theta^+(1540)$ state using the QCD sum rules framework. In Ref. [42] the QCD sum rules were employed to obtain the parity and the mass of the Θ^+ state. They obtained the parity as negative using the sum rules relativistic quantum theor with the standard values of condensates. In Ref. [43] again a QCD sum rules approach was performed for Θ^+ based on the proposal of Jaffe and Wilczek [30] but with a different current than the current of Ref. [41]. A study, using the QCD sum rules approach including OPE and direct instanton contribution, of triquark correlation was performed in Ref. [44] and it was shown that the direct instanton might be important for the pentaquarks. And again considering the direct instanton contributions Lee et al. [45] performed a full QCD sum rules calculation to determine mass and parity of the lowest lying pentaquark state which resulted in a positive parity for Θ^+

and a mass value $m_{\Theta^+} \simeq 1.7$ GeV. A QCD sum rules study of the decay of the Θ^+ pentaquark was presented in Ref. [46] using the diquark-diquark-antiquark scheme with one scalar and one pseudoscalar diquark. The application to the heavy pentaquarks was performed in a previous work [48], where a pentaquark current composed of two diquarks and an antiquark was used, and the sum rules consistent with a stable positive parity pentaquark state were found. A similar sum rules approach was also applied to the $D_s(2317)$ [49].

In this work, we extend the previous QCD sum rules calculations to investigate the anti-charmed pentaquark state with and without strangeness using two different currents for each case. We find a convergent Operator Product Expansion (OPE) only for the sum rules of the non-strange heavy pentaquark obtained with an interpolating field composed of two diquarks and one anti-charm quark, which was previously used in Ref. [48]. The stability of non-strange heavy pentaquark is consistent with the result based on the quark model with flavor spin interaction [38]. We then refine the convergent sum rules by explicitly including the DN (D meson-Nucleon) two-particle irreducible contribution. The importance of subtracting out such two-particle irreducible contribution was emphasized in Ref. [50, 51, 52] for the light pentaquark state. In these references it was pointed out that in the naive pentaquark correlation functions the exotic pentaquark interpolating current can couple to the meson-baryon scattering

states. For the Θ^+ pentaquark, the five quark current couples to the KN scattering state and this would contaminate the analysis of Θ^+ resonance. As a result the removal of the KN state is important to understand the properties of Θ^+ from QCD sum rules analysis. In fact, estimating the contribution from the lowest two-particle irreducible contribution is equally important in lattice gauge theory calculations [53, 54] to isolate the signal for the pentaquark state from the low-lying continuum state. We find that for the non-strange heavy pentaquark sum rules, including the DN continuum contribution tends to shift the position of the pentaquark state downwards. Given the negative experimental signatures of the charmed pentaquark states above the threshold, the present result suggests that the anti-charmed pentaquark states might be bound as was predicted in D meson bound soliton models.

This thesis is organized as follows. In Chapter 2, QCD sum rules will be discussed, throughout this discussion the Refs. [56, 58, 59, 60, 61, 62] will be followed. In Chapter 3, the QCD sum rules will be applied to the heavy pentaquark Θ_c , where we introduce the interpolating field for the Θ_c and discuss the dispersion relations that we will be using, and also the phenomenological side and the OPE side will be given in this chapter. In Chapter 4, the QCD sum rules for Θ_c and its numerical analysis will be given. And finally Chapter 5 is devoted to the conclusions.

CHAPTER 2

QCD SUM RULES

The QCD sum rules proposed by Shifman, Vainshtein, and Zakarov [55] proves to be very useful in understanding and extracting the hadron masses and coupling constants. It is a powerful nonperturbative framework in which one can connect various hadronic properties with the nonperturbative nature of QCD, which is represented by the vacuum condensates. Over the last decade QCD sum rules technique has been applied successfully and it has suggested that spectral properties of many hadrons can be determined in terms of a small number of quark and gluon condensates [55, 56, 57]. In this chapter a review of the most important features of the sum rules approach will be presented based on Refs. [56, 58, 59, 60, 61, 62].

2.1 QCD Sum Rules

In QCD sum rules one expresses various hadronic properties in terms of QCD parameters and studies the hadron corresponding to the lowest-mass state with

a given set of quantum number. For this purpose a time-ordered correlation function of interpolating fields, which is built from quark fields, is employed. The Fourier-transformed correlation function of interpolating field, or current $J(x)$ is given by

$$\Pi(q^2) = i \int d^4x e^{iqx} \langle 0 | T \{ J(x) \bar{J}(0) \} | 0 \rangle = \not{q} \Pi_q(q^2) + \Pi_1(q^2) , \quad (2.1)$$

where the $|0\rangle$ is the nonperturbative vacuum and T is the time ordering operator. $\Pi_q(q^2)$ and $\Pi_1(q^2)$ are called the chiral-even and chiral-odd parts, respectively. This correlation function is used to obtain the masses of the hadrons. $J(x)$ has the same quantum numbers as the hadron to be studied. One can have an interpolating field $J(x)$ which can be scalar, pseudoscalar, vector, spinor etc., depending on the quantum numbers of the hadron under consideration Eq. (2.1) is written for a spinor current.

When QCD sum rules method is considered the starting point is the construction of an interpolating field that carries the quantum numbers of the state concerned. An extremely good choice for such a field can be obtained by taking the constituent quark model as a base. An interpolating field which has the same valance quark content and quantum numbers, such as spin, isospin, parity as the hadron of interest, can be chosen. The interpolating field chosen for a state can also annihilate or create other resonances and continuum states with the same constituent quark content and quantum numbers. For instance, a Roper resonance and higher states are also annihilated (created) by the interpolating fields

of nucleon. All of these contribute to the correlation function. Therefore some other methods must be used to filter out the unwanted states. In order to do that, the mathematical operation which is known as the Borel transformation which will be explained in Subsection 2.5 is applied.

To calculate the correlation function which is given by Eq. (2.1) two methods are used: On the one hand, using the so-called operator product expansion (OPE) technique one can calculate the correlator in terms of QCD degrees of freedom when $q^2 \ll 0$. On the other hand, one can also calculate the correlation function phenomenologically with hadronic degrees of freedom.

QCD sum rules is obtained by equating the correlators calculated by the OPE and phenomenologically and it directly relates the spectral parameters, such as the masses and other parameters of the phenomenological ansatz, which is the low-lying resonance, to QCD Lagrangian parameters and condensates. Borel transformation improves the matching of the QCD and phenomenological descriptions.

In the following sections the general details of the QCD sum rules technique will be presented.

2.2 Phenomenological Representation and Dispersion Relation

One can calculate the correlator $\Pi(q^2)$ by inserting a complete set of physical intermediate state in Eq. (2.1), and one then obtains the following equation for the correlator

$$\Pi(q^2) = \sum_H \frac{\langle 0|J|H(p)\rangle\langle H(p)|\bar{J}|0\rangle}{q^2 - m_H^2}, \quad (2.2)$$

where the hadronic states $\{|H\rangle\}$ form a complete set. Here the interpolating field couples through

$$\langle 0|J|H(p)\rangle = \lambda_H u(p) \quad (2.3)$$

if H is spin- $\frac{1}{2}$ particle (such as the pentaquark), λ_H is called the residue or overlap, and $u(p)$ is a spinor. λ_H measures the coupling strength between the interpolating field and the physical state. Since the interpolating field $J(x)$ is an operator that annihilates (creates) all hadronic states whose quantum numbers and quark contents are same with $J(x)$ the information about all these hadronic states which also includes the low mass hadron of interest are contained in $\Pi(q^2)$. In this sense the correlator is analogous to a sum of propagators. In the narrow state approximation one can write the correlator as,

$$\begin{aligned} \Pi^{Phen}(q^2) = & -\frac{|\lambda_H|^2(\not{q} \pm m_H)}{q^2 - m_H^2 + i\varepsilon} - \frac{|\lambda_{H_1^*}|^2(\not{q} \pm m_{H_1^*})}{q^2 - m_{H_1^*}^2 + i\varepsilon} \\ & - \frac{|\lambda_{H_2^*}|^2(\not{q} \pm m_{H_2^*})}{q^2 - m_{H_2^*}^2 + i\varepsilon} + \dots, \end{aligned} \quad (2.4)$$

where the $+$ ($-$) sign is for positive (negative) parity state, m_{H_i} is the mass of the i^{th} resonance, λ_{H_i} is the coupling strenght of the i^{th} resonance to the interpolating

field, and ... denotes the contribution coming from the higher-mass states. More generally the correlator can be written as

$$\Pi_j^{Phen}(q^2) = - \int_0^\infty ds \frac{\rho_j^{Phen}(s)}{q^2 - s + i\varepsilon} + \dots \quad j = 1, q, \quad (2.5)$$

since in general these states occupy a continuous rather than a discrete spectrum. Here s is the particular invariant mass squared, $\rho_j^{Phen}(s)$ is the spectral density which contains the spectral properties of hadrons and ... denotes the subtraction terms which are polynomial in q^2 with unknown coefficients. From the Eq. (2.5), it is easy to verify that

$$\rho_j^{Phen}(s) = \frac{1}{\pi} \text{Im} \Pi_j^{Phen}(s), \quad (2.6)$$

and one immediately sees that the spectral densities for Eq. (2.4) are given as,

$$\rho_q^{Phen}(s) = |\lambda_H|^2 \delta(s - m_H^2) + |\lambda_{H_1^*}|^2 \delta(s - m_{H_1^*}^2) + |\lambda_{H_2^*}|^2 \delta(s - m_{H_2^*}^2) + \dots, \quad (2.7)$$

and

$$\begin{aligned} \rho_1^{Phen}(s) = & \mp |\lambda_H|^2 m_H \delta(s - m_H^2) \mp |\lambda_{H_1^*}|^2 m_{H_1^*} \delta(s - m_{H_1^*}^2) \\ & \mp |\lambda_{H_2^*}|^2 m_{H_2^*} \delta(s - m_{H_2^*}^2) + \dots. \end{aligned} \quad (2.8)$$

In order the QCD sum rules techniques to have predictive power, the phenomenological spectrum must be parameterized in a useful way. The effect of usually broader higher mass states in the spectrum will be eventually suppressed and the lowest resonance which is often fairly narrow will be emphasized. Therefore, the spectral density can, to a good approximation, be parameterized as

a single sharp pole representing the lowest resonance plus a smooth continuum representing higher states:

$$\begin{aligned}\rho_q^{Phen}(s) &= |\lambda_H|^2 \delta(s - m_H^2) + \rho^{Cont}(s) \\ \rho_1^{Phen}(s) &= \mp |\lambda_H|^2 m_H \delta(s - m_H^2) + \rho^{Cont}(s) .\end{aligned}\tag{2.9}$$

Note that this description is not perfect; but as one shall see, only weighted average of ρ_j^{Phen} is important in QCD sum rules. Thus, only the most prominent features of ρ_j^{Phen} are important; the detailed structures of ρ_j^{Phen} can not be resolved in sum rule calculations [60]. For simplicity it is assumed that the continuum contribution to the spectral density $\rho^{Cont}(s)$ vanish below a certain continuum threshold s_0 ; above this threshold one assumes the $\rho^{Cont}(s)$ to be given by the result obtained with OPE. This equivalence which is called the quark hadron duality is expected by the asymptotic freedom property of QCD for sufficiently large s . As a result the contribution to the spectral density which comes from the continuum is estimated as

$$\rho^{Cont}(s) = \rho^{OPE}(s) \Theta(s - s_0) .\tag{2.10}$$

Note that the choice of the s_0 , which is related to the 1st (or 2nd) excited resonance, is quite artificial. It is chosen considering that around these excited resonance regions the Borel stability is good (see Section 2.5). Since Eq. (2.10) is a phenomenological ansatz, the sensitivity of the prediction of sum rules to the choice of s_0 is necessarily checked.

2.3 Operator Product Expansion

Operator Product Expansion (OPE) which was first proposed by Wilson [63] intuitively, is essential for nonperturbative analysis in QCD sum rules. The main point is that one expands the time-ordered product of two nonlocal operators at short distance in terms of local operators which are multiplied by c-number coefficients. This expansion is

$$T[J(x)\bar{J}(0)] \stackrel{x \rightarrow 0}{\equiv} \sum_n c_n(x) \hat{O}_n . \quad (2.11)$$

The c -number coefficients are known as Wilson coefficients and information on the short-distance physics is contained in these coefficients. On the other hand the nonperturbative long-distance effects are contained in the local composite operators \hat{O}_n . As an example the collection of all the composite gauge invariant operators with dimension equal or less than six are given below

$$\begin{array}{ll} I & \text{(The unit operator)} \quad (d = 0) , \\ \bar{q}q & (d = 3) , \\ G_{\mu\nu}^a G^{a\mu\nu} & (d = 4) , \\ \bar{q}\sigma_{\mu\nu} G^{a\mu\nu} t^a q & (d = 5) , \\ \bar{q}\Gamma_1 q \bar{q}\Gamma_2 q & (d = 6) , \\ f_{abc} G_{\mu}^{a\nu} G_{\nu}^{b\lambda} G_{\lambda}^{c\mu} & (d = 6) . \end{array} \quad (2.12)$$

There are also other operators which are obtained by multiplying above operators by quark mass factors, such as $m_q \bar{q}q$. And also other dimension six operators such as $(D_\alpha G_{\mu\nu})(D_\beta G_{\rho\sigma})$, $(D_\alpha D_\beta G_{\mu\nu})G_{\rho\sigma}$ can be written in terms of the above operators via the equation of motion

$$D_\nu G_{\mu\nu} = g \sum_f \bar{q}_f \gamma_\mu t^a q_f . \quad (2.13)$$

After inserting Eq. (2.11) in Eq. (2.1) the two point correlation function will be,

$$\begin{aligned} \Pi(q^2) &= i \int d^4x e^{iqx} \sum_n c_n(x^2) \langle 0 | \hat{O}_n | 0 \rangle \\ &= \sum_n c_n(q^2) \langle 0 | \hat{O}_n | 0 \rangle . \end{aligned} \quad (2.14)$$

There is no dependence between the expansion Eq. (2.11) and the state in which the operator is evaluated. The Wilson coefficients of higher dimensional operators are suppressed by increasing powers of q^2 . Therefore, the operators with the lowest dimension are dominant and give power corrections to the perturbative contributions stemming from the unit operator.

The vacuum expectation matrix elements of \hat{O}_n are zero in perturbation theory, but in QCD the nature of the vacuum is changed by the nonperturbative effects (e.g. instantons) and nonvanishing vacuum expectation values are induced for these operators. From these matrix elements it can be deduced that nonperturbative effects modify the free particle propagator of quarks and gluons at large distances. OPE separates long distance and short distance contributions. Wilson coefficients contain short distance information and hence can be

calculated perturbatively using Feynman diagrammatic techniques.

An expression for the vacuum polarization $\Pi(q^2)$ is obtained in deep Euclidian region in terms of fundamental parameters of QCD and the matrix elements of \hat{O}_n in the physical nonperturbative vacuum of QCD after the calculation of Wilson coefficients. Then equating this expression to the physical representation via dispersion relation one obtains a relation between the parameters of the theory and hadron parameters. The dispersion relation for the OPE side is given as

$$\Pi_j^{OPE}(q^2) = - \int_0^\infty ds \frac{\rho_j^{OPE}(s)}{q^2 - s + i\varepsilon} + \dots \quad j = 1, q, \quad (2.15)$$

where $\rho^{OPE}(s)$ is the spectral density for the OPE side defined as

$$\rho_j^{OPE}(s) = \frac{1}{\pi} \text{Im} \Pi_j^{OPE}(s), \quad (2.16)$$

and ... denote the subtraction terms.

2.4 Analytic Continuation

As discussed earlier $\Pi^{OPE}(q^2)$ is valid in $q^2 \rightarrow -\infty$ region. On the other hand, $\Pi^{Phen}(q^2)$ is valid around $q^2 \sim$ resonance region. Therefore one needs to apply the analytic continuation to $\Pi^{OPE}(q^2)$ in order to match these two expressions.

In the case of the correlation function Eq. (2.1) one is allowed to perform the contour integral in Fig. 2.1 using the Cauchy formula for the analytic function $\Pi(q^2)$,

$$\begin{aligned}
\Pi(q^2) &= \frac{1}{2\pi i} \oint_C dz \frac{\Pi(z)}{z - q^2} \\
&= \frac{1}{2\pi i} \oint_{|z|=R} dz \frac{\Pi(z)}{z - q^2} \\
&\quad + \frac{1}{2\pi i} \int_0^R dz \frac{\Pi(z + i\epsilon) - \Pi(z - i\epsilon)}{z - q^2} , \tag{2.17}
\end{aligned}$$

where one can put the radius R of the contour to infinity which simplifies the right hand side of the Eq. (2.17) considerably, since if the correlation function vanishes sufficiently fast at $|q^2| \sim R \rightarrow \infty$, the integral over the circle tends to zero. The second integral on the right hand side of the Eq. (2.17) can be replaced by an integral over the imaginary part of $\Pi(q^2)$ making use of the Schwartz reflection principle: $\Pi(q^2 + i\epsilon) - \Pi(q^2 - i\epsilon) = 2i \operatorname{Im}\Pi(q^2)$ if $\Pi(q^2)$ is real on the negative q^2 axis [62], so the dispersion relation results in

$$\Pi_j^{OPE}(Q^2) = \int_0^\infty ds \frac{\rho_j^{OPE}(s)}{s + Q^2} + (\text{subtraction terms}) , \tag{2.18}$$

where $\Pi_j^{OPE}(Q^2) = \Pi_j^{OPE}(q^2)$ for $Q^2 = -q^2$, and $\rho_j^{OPE}(s)$ is defined as in Eq. (2.16). The subtraction terms which are polynomials in q^2 are the result of the circular integral at infinity.

2.5 Borel Transform And Sum Rules

So far we have two expression for the correlation function: one $\Pi^{Phen}(q^2)$ in terms of physical parameters, as discussed in Sec. 2.1, and the other one $\Pi^{OPE}(q^2)$ a theoretical expression which is a function of q^2 , α_s , the quark masses and the

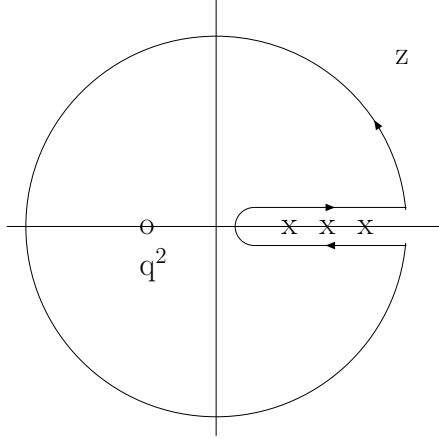


Figure 2.1: The contour in the plane of the complex variable $q^2 = z$. The open point indicates the $q^2 < 0$ reference point of the QCD calculations and the crosses indicates the positions of hadronic thresholds at $q^2 > 0$ [62].

vacuum expectation values of the operators \hat{O}_n . At this point one might attempt to match these two descriptions of the correlator; however such a matching is not yet practical. If one consider the OPE side, the contribution from higher dimensional operators are not sufficiently suppressed, and if the phenomenological side is considered, the spectrum is not sufficiently dominated by the lowest pole. In another words, one can only make a valid QCD expansion at sufficiently large spacelike q^2 , on the other hand one can obtain the phenomenological description which is significantly dominated by the lowest pole only for sufficiently small q^2 or better yet timelike q^2 near the lowest-mass state. Hence it is not yet possible to obtain information on the lowest-mass state.

Therefore besides analytic continuation, Borel transformation is often used to

improve the reliability of the sum rule and the overlap of the OPE and phenomenological description . The Borel transformation for a given function $f(Q^2)$ is defined as

$$f(Q^2) \rightarrow \tilde{f}(M^2) = \hat{L}^{-1} f(Q^2) = \lim_{Q^2, n \rightarrow \infty} \frac{(Q^2)^n}{(n-1)!} \left(\frac{-d}{dQ^2} \right)^n f(Q^2) , \quad (2.19)$$

$$Q^2 \equiv -q^2, \quad M^2 \equiv \frac{Q^2}{n} (= \text{finite}) , \quad (2.20)$$

where M is known as the Borel mass. In the QCD sum rules approach, the Borel transforms of the OPE and the phenomenological correlation function are equated

$$\Pi_j^{OPE}(M^2) = \Pi_j^{Phen}(M^2) . \quad (2.21)$$

At this point we can express the advantages attained by Borel transformation in QCD sum rules. First of all the polynomial terms appearing in the dispersion relation Eq. (2.5) are removed by Borel transformation. For the phenomenological side Borel transformation application leads to emphasis upon contribution from the lightest resonance. On the phenomenological side the correlator has a form

$$\Pi_j^{Phen}(Q^2) = \int_0^\infty ds \frac{\rho_j^{Phen}(s)}{s + Q^2} , \quad (2.22)$$

and therefore, for spacelike momentum, a power law suppresses the higher-mass states. On the other hand Borel-transformed correlator is given by

$$\Pi_j^{Phen}(M^2) = \int_0^\infty ds e^{-\frac{s}{M^2}} \rho_j^{Phen}(s) ; \quad (2.23)$$

which shows Borel transform changes a power suppression to an exponential suppression.

If the OPE side of the correlation function is considered, the Borel transformation also improves the convergence of this side. The nonperturbative part of the OPE of the correlation function is of the form

$$\Pi_{nonpert.}^{OPE}(Q^2) = \sum_{nonpert.} \frac{c'_n}{(Q^2)^n} \langle \hat{O}_n \rangle . \quad (2.24)$$

After the Borel transformation, one obtains

$$\Pi_{nonpert.}^{OPE}(M^2) = \sum_{nonpert.} \frac{c'_n}{(n-1)!(M^2)^n} \langle \hat{O}_n \rangle . \quad (2.25)$$

So higher dimensional terms which corresponds to higher n values are suppressed by a factorial factor while in Eq. (2.24) they are only suppressed as a simple power law in Q^2 .

In principle, M^2 is completely arbitrary and the physical parameters should be independent of M^2 , however in practice some moderate range of M^2 must be chosen. Actually, in the phenomenological side, if $M^2 \rightarrow 0$, the Borel transformed correlator is dominated most strongly by the lowest pole, while $M^2 \rightarrow \infty$ guarantees better convergence in the OPE side. Therefore an intermediate region in M^2 , where the contributions from the higher-dimensional operators and the higher-mass resonance are simultaneously suppressed to a sufficient degree, is usually chosen.

Given the form of OPE correlator in Eq. (2.18), the correlator for OPE side

under Borel transformation is given as

$$\Pi_j^{OPE}(M^2) = \int_0^\infty ds e^{-\frac{s}{M^2}} \rho_j^{OPE}(s) , \quad (2.26)$$

and the sum rule takes the form

$$\int_0^\infty ds e^{-\frac{s}{M^2}} \rho_j^{OPE}(s) = \int_0^\infty ds e^{-\frac{s}{M^2}} \rho_j^{Phen}(s) . \quad (2.27)$$

If the spectrum is parameterized as in Eq. (2.9) and Eq. (2.10) then the sum rules becomes

$$\int_0^{s_0} ds e^{-\frac{s}{M^2}} \rho_j^{OPE}(s) = \int_0^{s_0} ds e^{-\frac{s}{M^2}} \rho_j^{Phen}(s) . \quad (2.28)$$

2.6 Vacuum Condensates

To obtain the hadronic parameters such as mass and coupling strength from the QCD sum rules, the vacuum condensates which are the nonvanishing expectation values of composite operators given in Eq. (2.12), have to be known. In this section standard estimates of vacuum condensates will be reviewed. Because of the Lorentz invariance of the vacuum state $|0\rangle$ only spin-0 operators can have nonvanishing vacuum expectation values. Here we will deal only with the condensates that will be used in the next chapter.

Firstly the quark condensate $\langle \bar{q}q \rangle$ will be considered. It follows from the isospin symmetry that

$$\langle \bar{q}q \rangle = \langle \bar{u}u \rangle = \langle \bar{d}d \rangle . \quad (2.29)$$

One can determine the value of $\langle \bar{q}q \rangle$ from the Gell-Mann-Oakes-Renner relation,

$$(m_u + m_d)\langle \bar{q}q \rangle = -m_\pi^2 f_\pi^2 [1 + O(m_\pi^2)] , \quad (2.30)$$

where m_π and f_π denotes the pion mass and pion decay constant, and m_u and m_d are the up and down current quark masses. The value of the quark condensate can be determined at a particular renormalization scale if the values of the current quark masses are given at that same scale, since both sides of Eq. (2.30) are renormalization-group invariant [64]. If the experimental values for m_π and f_π are taken as 138 MeV and 93 MeV respectively and the standard values of the light quark masses are used it is obtained that $m_u + m_d = 14 \pm 4$ MeV at a renormalization scale of 1 GeV [65]. Therefore, the value for the $\langle \bar{q}q \rangle$ condensate is obtained as

$$\langle \bar{q}q \rangle \simeq -(0.225 \pm 0.025 \text{ GeV})^3 \quad (2.31)$$

at the renormalization scale of 1 GeV [65]. The strange quark condensate value is most often parameterized in terms of the up and down quark condensate as

$$\langle \bar{s}s \rangle = (1 + \bar{\gamma}_s)\langle \bar{q}q \rangle , \quad (2.32)$$

The $\bar{\gamma}_s$ value is estimated using the strange baryon sum rule as [56, 66, 67]

$$\bar{\gamma}_s \simeq -0.2 . \quad (2.33)$$

The first estimation of the gluon condensate is obtained from an analysis of leptonic decays of ϱ^0 and ϕ^0 mesons [68] and from a sum-rule analysis of the

charmonium spectrum [55] whose value is given as [69]

$$\langle \frac{\alpha_s}{\pi} G^2 \rangle \simeq (0.33 \pm 0.04 \text{ GeV})^4 . \quad (2.34)$$

Isospin symmetry implies for dimension five operators

$$\langle g_s \bar{u} \sigma . G u \rangle \simeq \langle g_s \bar{d} \sigma . G d \rangle \equiv \langle g_s \bar{q} \sigma . G q \rangle . \quad (2.35)$$

The quark-gluon condensate $\langle g_s \bar{q} \sigma . G q \rangle$ is given in terms of the quark condensate $\langle \bar{q} q \rangle$ as

$$\langle g_s \bar{q} \sigma . G q \rangle = 2 \langle \bar{q} D^2 q \rangle \equiv 2 \lambda_q^2 \langle \bar{q} q \rangle . \quad (2.36)$$

Here the first equality is obtained by using

$$G_{\mu\nu}^a = \frac{i}{g_s} [D_\mu, D_\nu]^a , \quad (2.37)$$

and the equations of motion

$$\begin{aligned} (i \not{D} - m_f) q_f &= 0 , \\ \bar{q}_f (i \overleftarrow{\not{D}} + m_f) &= 0 . \end{aligned} \quad (2.38)$$

In the QCD vacuum the average vacuum gluon field and the average virtuality (momentum squared) of the quarks are parameterized by the λ_q^2 and the value of this quantity is estimated as $\lambda_q^2 = 0.4 \pm 0.1 \text{ GeV}^2$ by the standard QCD sum rule [66, 70]. Lattice calculation [71], and QCD sum rule analysis of the pion form factor using nonlocal quark and gluon condensates [72] give larger values for λ_q^2 which are $\lambda_q^2 = 0.55 \pm 0.05 \text{ GeV}^2$ and $\lambda_q^2 = 0.7 \pm 0.1 \text{ GeV}^2$, respectively.

Having estimated the value of $\bar{\gamma}$ from strange baryon sum rules [66, 67] which is

$$\bar{\gamma}_g \simeq -0.2 , \quad (2.39)$$

quark-gluon condensate is parameterized as

$$\langle g_s \bar{s} \sigma . G s \rangle = (1 + \bar{\gamma}_g) \langle g_s \bar{q} \sigma . G q \rangle . \quad (2.40)$$

In QCD sum rule applications, one usually approximates the four quark condensates in terms of $\langle \bar{q} q \rangle$ and $\langle \frac{\alpha_s}{\pi} G^2 \rangle$ via factorization, or vacuum saturation, approximation. In this approximation one inserts a complete set of intermediate states in the middle of four-quark matrix element, but keeps only the dominant vacuum intermediate state. A more detailed discussion of the factorization approximation and estimation of four-quark condensates at finite density can be found in Ref. [73].

Using the dilute instanton gas approximation [55] the three-gluon condensate can be expressed in terms of two-gluon condensate as

$$\langle g_s^3 f G^3 \rangle \simeq \frac{48\pi^2}{5} \rho_c^{-2} \langle \frac{\alpha_s}{\pi} G^2 \rangle , \quad (2.41)$$

where the instanton size cutoff is $\rho_c \sim (200 \text{ MeV})^{-1}$. This instanton-based estimate and phenomenological estimate which is $\langle g_s^3 f G^3 \rangle \simeq 0.06 \text{ GeV}^6$ are well in agreement.

In practice, factorization assumption is used to determine the values of condensates with dimension $d_m \geq 7$ since there is no reliable way to estimate their

values. So one can make effective estimations for the higher-dimensional condensates in terms of the lower-dimensional condensates. In many cases of the sum rule applications, the Borel transformed OPE converges quickly and one expects negligible contribution from the higher dimensional condensates.

CHAPTER 3

QCD SUM RULES FOR ANTICHARMED PENTAQUARK Θ_c

In this chapter, the sum rules to obtain the mass and parity of the Θ_c pentaquark will be established following the method discussed in Chapter 2. In the OPE for Θ_c pentaquark correlator, contribution from all condensates up to dimension twelve, and the terms up to first order in the strange quark mass m_s are included. The contribution coming from the up and down current quark masses are neglected since they give numerically small contribution.

3.1 Interpolating Field for Θ_c

One of the requirements of the QCD sum rule approach is the introduction of an interpolating field having strong overlap with the hadron which is dealt with. For this purpose, for the QCD sum rule analysis of anticharmed pentaquark state Θ_c , which has no strangeness, the following two interpolating fields are introduced:

$$\Theta_{c1} = \epsilon^{abc}(u_a^T C \gamma_\mu u_b) \gamma_5 \gamma_\mu d_c (\bar{c}_d i \gamma_5 d_d) ,$$

$$\Theta_{c2} = \epsilon^{abk}(\epsilon^{aef}u_e^T C \gamma_5 d_f)(\epsilon^{bgh}u_g^T C d_h) C \bar{c}_k^T . \quad (3.1)$$

Here the roman indices a, b, \dots are color indices, C denotes charge conjugation, and T denotes transpose. It is important to notice that Θ_{c1} is composed of a nucleon current (*proton*) and a pseudo scalar current (D meson), on the other hand Θ_{c2} which has been investigated by H. Kim et al. [48] in a previous work, is composed of diquark-diquark-antiquark.

For the charmed pentaquark with strangeness, we consider the following two possible currents,

$$\begin{aligned} \Theta_{cs1} &= \epsilon^{abk}(\epsilon^{aef}u_e^T C s_f)(\epsilon^{bgh}u_g^T C d_h) C \bar{c}_k^T , \\ \Theta_{cs2} &= \epsilon^{abk}(\epsilon^{aef}u_e^T C \gamma_5 s_f)(\epsilon^{bgh}u_g^T C d_h) C \bar{c}_k^T . \end{aligned} \quad (3.2)$$

Here, instead of choosing Θ_{cs1} as a direct product of a nucleon and a D_s meson or a hyperon and a D meson currents as in Θ_{c1} , we choose it to well represent a state having two diquark structure with the same scalar quantum number but with different flavor. Such configuration allows all the five constituent quarks to be in the s -wave states, which will have the lowest orbital energy and consequently could be the dominant ground state configuration [29]. Moreover, as it will be seen, Θ_{c1} couples dominantly to the nucleon and D meson state, suggesting that currents composed of a direct product of a nucleon and a meson currents are not suitable for investigating the properties of the pentaquark state.

Under parity transformation $q'(x') = \gamma_0 q(x)$ where $x' = (x_0, -\vec{x})$, the Θ_{c1}

currents transform as,

$$\begin{aligned}
\Theta'_{c1} &= \epsilon^{abc} (u_a'^T C \gamma_\mu u_b') \gamma_5 \gamma_\mu d_c' (\bar{c}'_d i \gamma_5 d_d') , \\
&= \epsilon^{abc} ((\gamma_0 u_a)^T C \gamma_\mu \gamma_0 u_b) \gamma_5 \gamma_\mu \gamma_0 d_c (\overline{(\gamma_0 c_d)} i \gamma_5 \gamma_0 d_d) ,
\end{aligned} \tag{3.3}$$

which, after a little algebra, becomes:

$$\begin{aligned}
\Theta'_{c1} &= -\gamma_0 \epsilon^{abc} (u_a^T C \gamma_\mu u_b) \gamma_5 \gamma_\mu d_c (\bar{c}_d i \gamma_5 d_d) \\
&= -\gamma_0 \Theta_{c1} .
\end{aligned} \tag{3.4}$$

Parity transformation of the other currents can be obtained similarly and under the parity transformation, the Θ_c currents transform as

$$\begin{aligned}
\Theta'_{c1} &= -\gamma_0 \Theta_{c1} , \\
\Theta'_{c2} &= \gamma_0 \Theta_{c2} , \\
\Theta'_{cs1} &= -\gamma_0 \Theta_{cs1} , \\
\Theta'_{cs2} &= \gamma_0 \Theta_{cs2} .
\end{aligned} \tag{3.5}$$

3.2 Dispersion Relation

In this calculation two types of QCD sum rules will be used. The first type of QCD sum rules for the heavy pentaquarks that we will be using are constructed from the time ordered correlation function, whose form is given in Chapter 2:

$$\Pi_T(q) = i \int d^4x e^{iq \cdot x} \langle 0 | T[\Theta_c(x), \bar{\Theta}_c(0)] | 0 \rangle \equiv \Pi_1(q^2) + \not{q} \Pi_q(q^2) , \tag{3.6}$$

where Θ_c can be any of the currents in Eq. (3.1) or in Eq. (3.2), and Π_q , Π_1 are called the chiral even and chiral odd parts respectively. As can be seen in Eq. (3.5), the currents are not eigenstates of the parity transformation and can couple to both positive and negative parity states. The spectral densities calculated from the OPE of Eq. (3.6) are matched to that obtained from the phenomenological assumption in the Borel-weighted dispersion integral,

$$\int_{m_c^2}^{s_0} dq^2 e^{-q^2/M^2} W(q^2) \frac{1}{\pi} \text{Im}[\Pi_i^{\text{phen}}(q^2) - \Pi_i^{\text{ope}}(q^2)] = 0, \quad (i = 1, q), \quad (3.7)$$

where M^2 is the Borel mass. Here, higher resonance contributions are subtracted according to the QCD duality assumption, which introduces the continuum threshold s_0 . In this equation an additional weight function $W(q^2)$ have also been introduced for later use.

The second type of QCD sum rule that we will be using in this work is the “old-fashioned” correlation function, which is defined as [42]

$$\Pi_T(q) = i \int d^4x e^{iq \cdot x} \langle 0 | \theta(x^0) \Theta_c(x) \bar{\Theta}_c(0) | 0 \rangle. \quad (3.8)$$

Positive and negative parity states can be separated using the technique given in [74] for the ordinary three quark baryons and this type of correlation function has been used in projecting out positive and negative parity nucleon states [74]. To separate the positive-parity and negative parity baryons the correlation function Eq. (3.8) is used. In the zero-width resonance approximation, the imaginary

part in the rest frame $\vec{q} = 0$ is written as

$$\begin{aligned} \frac{1}{\pi} \text{Im} \Pi(q_0) &= \sum_H \left[(\lambda_H^+)^2 \frac{\gamma_0 + 1}{2} \delta(q_0 - m_H^+) + (\lambda_H^-)^2 \frac{\gamma_0 - 1}{2} \delta(q_0 - m_H^-) \right] \\ &\equiv A(q_0) \gamma^0 + B(q_0) , \end{aligned} \quad (3.9)$$

where λ_H^+ (λ_H^-) is the coupling strenght between the interpolating field and the physical state with the positive-parity (negative-parity), and $A(q_0)$ and $B(q_0)$ are defined as

$$\begin{aligned} A(q_0) &= \frac{1}{2} \sum_H [(\lambda_H^+)^2 \delta(q_0 - m_H^+) + (\lambda_H^-)^2 \delta(q_0 - m_H^-)] , \\ B(q_0) &= \frac{1}{2} \sum_H [(\lambda_H^+)^2 \delta(q_0 - m_H^+) - (\lambda_H^-)^2 \delta(q_0 - m_H^-)] . \end{aligned} \quad (3.10)$$

It can be seen that the combination $A(q_0) + B(q_0)$ [$A(q_0) - B(q_0)$] contains the contribution only from the positive-parity (negative-parity) states. So the imaginary part is divided into the following two parts, which are defined only for $q_0 > 0$,

$$\frac{1}{\pi} \text{Im} \Pi(q_0) = A(q_0) \gamma^0 + B(q_0) . \quad (3.11)$$

One should note that these can be identified with the imaginary part calculated from Eq. (3.6),

$$\begin{aligned} A(q_0) &= \frac{1}{\pi} \text{Im} \Pi_q(q_0) q_0 \\ B(q_0) &= \frac{1}{\pi} \text{Im} \Pi_1(q_0) , \end{aligned} \quad (3.12)$$

for $q_0 > 0$.

Now, depending on the parity of the current Θ_c in Eq. (3.5), one can extract the positive or negative-parity physical state only by either adding or subtracting A and B . That is, the spectral density for the positive and negative parity physical states will be as follows,

$$\rho^\pm(q_0) = \begin{cases} A(q_0) \mp B(q_0) & \text{For } \Theta_{c1}, \Theta_{cs1} \\ A(q_0) \pm B(q_0) & \text{For } \Theta_{c2}, \Theta_{cs2} \end{cases}. \quad (3.13)$$

The sum rules are then obtained by again matching the corresponding spectral density from the OPE and phenomenological side,

$$\int_0^\infty dq_0 e^{-q_0^2/M^2} [\rho_{\text{phen}}^\pm(q_0) - \rho_{\text{oep}}^\pm(q_0)] = 0. \quad (3.14)$$

3.3 Phenomenological Side

3.3.1 Θ_{c1} and Θ_{cs1}

For Θ_{c1} current, the interpolating field couples to a positive parity state as,

$$\langle 0 | \Theta_{c1}(x) | \Theta_c(\mathbf{p}) : P = + \rangle = \lambda_{+,c1} \gamma_5 U_\Theta(\mathbf{p}) e^{-ip \cdot x}, \quad (3.15)$$

and to a negative parity state as,

$$\langle 0 | \Theta_{c1}(x) | \Theta_c(\mathbf{p}) : P = - \rangle = \lambda_{-,c1} U_\Theta(\mathbf{p}) e^{-ip \cdot x}. \quad (3.16)$$

Here, $\lambda_{\pm,c1}$ denotes the coupling strength between the interpolating field and the physical state with the specified parity and $U(\mathbf{p})$ is the spinor of the pentaquark with momentum \mathbf{p} . Similar relations will hold for Θ_{cs1} . Using these, we obtain

the phenomenological side of Eq. (3.6) separated into chiral even (Π_q) and odd (Π_1) parts, which are defined to be the parts proportional to \not{q} and 1 respectively.

As was first pointed out in Ref. [50], the correlation function can also couple to the DN (D meson-Nucleon) continuum state, whose threshold could be lower than the expected Θ_c mass. Its phenomenological contribution can be estimated by using,

$$\langle 0 | \Theta_{c1} | DN(\mathbf{p}) \rangle = i \lambda_{DN,c1} U_N(\mathbf{p}) . \quad (3.17)$$

Combining these two contributions, we find

$$\begin{aligned} \Pi_{T,c1}^{\text{phen}}(q) = & -|\lambda_{\pm,c1}|^2 \frac{\not{q} \mp m_{\Theta}}{q^2 - m_{\Theta}^2} \\ & -i|\lambda_{DN,c1}|^2 \int d^4p \frac{(\not{p} + m_N)}{p^2 - m_N^2} \frac{1}{(p-q)^2 - m_D^2} + \dots, \end{aligned} \quad (3.18)$$

where the minus (plus) sign in front of m_{Θ} is for positive (negative) parity. The dots denote higher resonance contributions that should be parameterized according to QCD duality. It should be noted however that higher resonances with different parities contribute differently to the chiral-even and chiral odd parts [75]. Thus, Π_q^{phen} and Π_1^{phen} constitute separate sum rules. For Θ_{cs1} , the D meson should be replaced by the D_s meson.

Spectral density for DN can be obtained from the second part of the right hand side of the Eq. (3.18) which is given as

$$\begin{aligned} \Pi_{T,c1}^{\text{phen,DN}}(q) = & -i|\lambda_{DN,c1}|^2 \int d^4p \frac{(\not{p} + m_N)}{p^2 - m_N^2} \frac{1}{(p-q)^2 - m_D^2} \\ = & \not{q} \Pi_q^{DN}(q) + \Pi_1^{DN}(q) . \end{aligned} \quad (3.19)$$

If the trace of Eq. (3.19) is calculated the equation for $\Pi_1^{DN}(q)$ is obtained as

$$\begin{aligned}\Pi_1^{DN}(q) &= \frac{1}{4}Tr[\Pi_{T,c1}^{\text{phen},DN}(q)] \\ &= \frac{-i}{4}|\lambda_{DN,c1}|^2 \int d^4p \frac{1}{p^2 - m_N^2} \frac{1}{(p-q)^2 - m_D^2} Tr[\not{p} + m_N] ,\end{aligned}\quad (3.20)$$

and again after multiplying Eq. (3.19) by \not{q} and then calculating the trace of it the equation for $\Pi_q^{DN}(q)$ is obtained as

$$\begin{aligned}\Pi_q^{DN}(q) &= \frac{1}{4q^2}Tr[\not{q}\Pi_{T,c1}^{\text{phen},DN}(q)] \\ &= \frac{-i}{4q^2}|\lambda_{DN,c1}|^2 \int d^4p \frac{1}{p^2 - m_N^2} \frac{1}{(p-q)^2 - m_D^2} \\ &\quad \times Tr[\not{q} \not{p} + \not{q} m_N] .\end{aligned}\quad (3.21)$$

After calculating the traces one takes the imaginary part of the Eq. (3.20) and Eq. (3.21) and calculates the four dimensional integrals in these equations to obtain the spectral density for DN contribution.

The corresponding spectral density for the pole and DN contributions are given respectively by

$$\begin{aligned}\frac{1}{\pi}\text{Im}\Pi_{T,c1}^{\text{pole}}(q) &= \not{q}|\lambda_{\pm,c1}|^2\delta(q^2 - m_\Theta^2) \mp m_\Theta|\lambda_{\pm,c1}|^2\delta(q^2 - m_\Theta^2), \\ \frac{1}{\pi}\text{Im}\Pi_{T,c1}^{DN}(q) &= \not{q}|\lambda_{DN,c1}|^2 \frac{q^2 + m_N^2 - m_D^2}{32\pi^2 q^4} \\ &\quad \times \sqrt{q^4 - 2q^2(m_N^2 + m_D^2) + (m_N^2 - m_D^2)^2} \\ &\quad + |\lambda_{DN,c1}|^2 \frac{2m_N}{32\pi^2 q^2} \\ &\quad \times \sqrt{q^4 - 2q^2(m_N^2 + m_D^2) + (m_N^2 - m_D^2)^2} .\end{aligned}\quad (3.22)$$

We notice that the chiral-odd part has opposite sign depending on the parity while the chiral even part has positive-definite coefficient.

3.3.2 Θ_{c2} and Θ_{cs2}

As can be seen in Eq. (3.5), Θ_{c2} transforms differently compared to Θ_{c1} under parity. Thus, the couplings to the interpolating field are

$$\begin{aligned}\langle 0|\Theta_{c2}(x)|\Theta_c(\mathbf{p}) : P = + \rangle &= \lambda_{+,c2} U_\Theta(\mathbf{p}) e^{-ip \cdot x} , \\ \langle 0|\Theta_{c2}(x)|\Theta_c(\mathbf{p}) : P = - \rangle &= \lambda_{-,c2} \gamma_5 U_\Theta(\mathbf{p}) e^{-ip \cdot x} .\end{aligned}\quad (3.23)$$

Similarly, the coupling to the DN continuum state changes as follows,

$$\langle 0|\Theta_{c2}|DN(\mathbf{p}) \rangle = \lambda_{DN,c2} \gamma_5 U_N(\mathbf{p}) . \quad (3.24)$$

Combining these changes, we find,

$$\begin{aligned}\Pi_{T,c2}^{\text{phen}}(q) &= -|\lambda_{\pm,c2}|^2 \frac{\not{q} \pm m_\Theta}{q^2 - m_\Theta^2} \\ &\quad + i|\lambda_{DN,c2}|^2 \int d^4p \frac{\gamma_5(\not{p} + m_N)\gamma_5}{p^2 - m_N^2} \frac{1}{(p-q)^2 - m_D^2} + \dots\end{aligned}\quad (3.25)$$

Consequently, the spectral densities, which are obtained following the same steps as the Θ_{c1} and Θ_{cs1} case, are

$$\begin{aligned}\frac{1}{\pi} \text{Im} \Pi_{T,c2}^{\text{pole}}(q) &= \not{q} |\lambda_{\pm,c2}|^2 \delta(q^2 - m_\Theta^2) \pm m_\Theta |\lambda_{\pm,c2}|^2 \delta(q^2 - m_\Theta^2), \\ \frac{1}{\pi} \text{Im} \Pi_{T,c2}^{\text{DN}}(q) &= \not{q} |\lambda_{DN,c2}|^2 \frac{q^2 + m_N^2 - m_D^2}{32 \pi^2 q^4} \\ &\quad \times \sqrt{q^4 - 2q^2(m_N^2 + m_D^2) + (m_N^2 - m_D^2)^2}\end{aligned}$$

$$\begin{aligned}
& -|\lambda_{DN,c2}|^2 \frac{2m_N}{32\pi^2 q^2} \\
& \times \sqrt{q^4 - 2q^2(m_N^2 + m_D^2) + (m_N^2 - m_D^2)^2} . \quad (3.26)
\end{aligned}$$

3.3.3 Final Form of the Phenomenological Side

The final form for the phenomenological side to be used in Eq. (3.14) can be obtained from combining Eq. (3.22) or Eq. (3.26) according to Eq. (3.13), both of which are given in the following form,

$$\begin{aligned}
\rho_{\text{phen}}^{\pm}(q_0) = & |\lambda_{\pm}|^2 \delta(q_0 - m_{\Theta}) + \theta(\sqrt{s_0} - q_0) \rho_{DN}^{\pm}(q_0) \\
& + \theta(q_0 - \sqrt{s_0}) \rho_{\text{cont}}^{\pm}(q_0) , \quad (3.27)
\end{aligned}$$

where the usual duality assumption has been used to represent the higher resonance contribution above the continuum threshold $\sqrt{s_0}$; i.e., $\rho_{\text{cont}}^{\pm}(q_0) = \rho_{\text{ope}}^{\pm}(q_0)$.

The spectral density for the two-particle irreducible part is given by

$$\begin{aligned}
\rho_{DN,c1}^{\pm}(q_0) = & \frac{|\lambda_{DN,c1}|^2}{32\pi^2} \sqrt{(q_0 - m_D)^2 - m_N^2} \sqrt{(q_0 + m_D)^2 - m_N^2} \\
& \times \frac{(q_0 \pm m_N)^2 - m_D^2}{q_0^3} , \quad (3.28)
\end{aligned}$$

$$\begin{aligned}
\rho_{DN,c2}^{\pm}(q_0) = & \frac{|\lambda_{DN,c2}|^2}{32\pi^2} \sqrt{(q_0 - m_D)^2 - m_N^2} \sqrt{(q_0 + m_D)^2 - m_N^2} \\
& \times \frac{(q_0 \mp m_N)^2 - m_D^2}{q_0^3} . \quad (3.29)
\end{aligned}$$

We substitute the above into the Borel transformed dispersion relation in Eq. (3.14).

3.4 OPE Side

3.4.1 The OPE for Θ_{c1}

In this section we present the result of the OPE calculation for Θ_{c1} . We use the momentum-space expression for the charm quark propagator and we keep the charm quark mass finite. For the light quark part of the correlation function, we calculate in the coordinate-space, which is then Fourier-transformed to the momentum space in D -dimension. The resulting light-quark part is combined with the charm-quark part before it is dimensionally regularized at $D = 4$.

Our OPE is given by

$$\begin{aligned} \Pi^{\text{ope},c1}(q) = & \Pi^{(a)} + \Pi^{(b)} + \Pi^{(c)} + \Pi^{(d)} + \Pi^{(e)} \\ & + \Pi^{(f)} + \Pi^{(g)} + \Pi^{(h)} + \Pi^{(i)} + \Pi^{(j)}, \end{aligned} \quad (3.30)$$

where the superscripts indicate each diagram in Fig. 3.1. At this part firstly the detailed calculation for the Diagram (a) in Fig. 3.1 will be given. For the Diagram (a), which represents the perturbative contribution, one obtains

$$\begin{aligned} \Pi^{(a)}(q^2) = & i \int d^4x e^{iq \cdot x} \langle 0 | T \{ [\epsilon^{abc} u_a^\alpha(x) (C \gamma_\mu)^{\alpha\beta} u_b^\beta(x) (\gamma_5 \gamma_\mu)^{\delta\sigma} \\ & \times d_c^\sigma(x) \bar{c}_d^\tau(x) (i \gamma_5)^{\tau\theta} d_d^\theta(x)] [-\epsilon^{a'b'c'} \bar{d}_{c'}^{\sigma'}(0) (\gamma_{\mu'} \gamma_5)^{\sigma'\delta'} \\ & \times \bar{u}_{b'}^{\beta'}(0) (\gamma_{\mu'} C)^{\beta'\alpha'} \bar{u}_{a'}^{\alpha'}(0) \bar{d}_{d'}^{\theta'}(0) (i \gamma_5)^{\theta'\tau'} c_{d'}^{\tau'}(0)] \} | 0 \rangle \end{aligned} \quad (3.31)$$

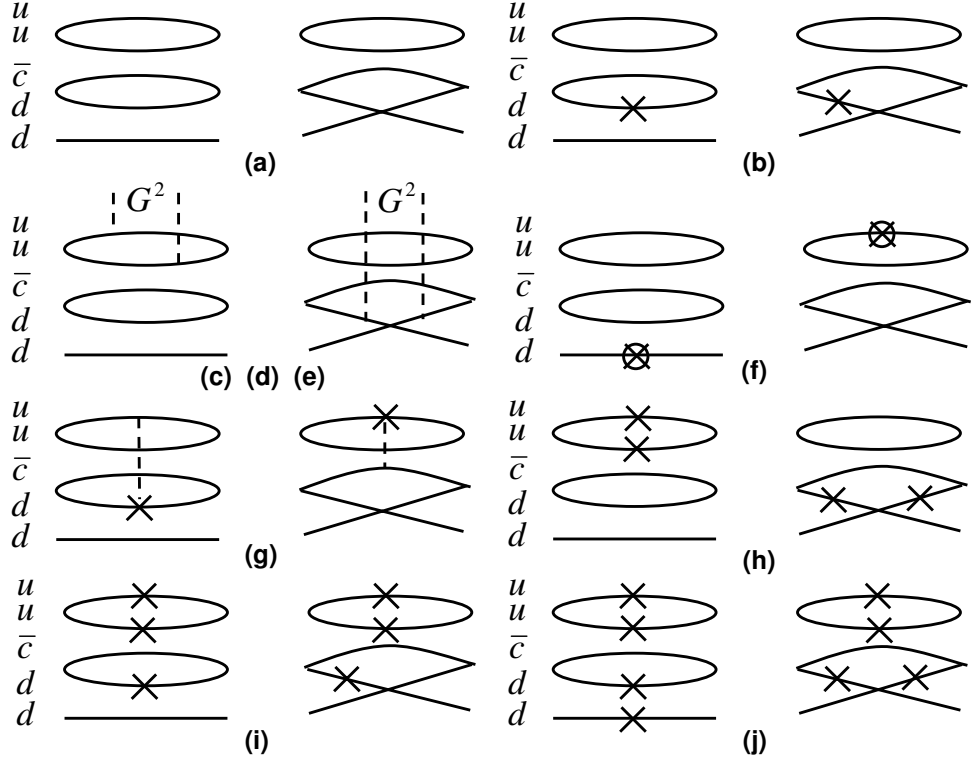


Figure 3.1: Schematic OPE diagrams for the current Θ_{c1} in Eq. (3.2). Each label corresponds to that in Eq. (3.41). The solid lines denote quark (or anti-charm quark) propagators and the dashed lines are for gluon. The crosses denote the quark condensate, and the crosses with circle represent the mixed quark gluon condensates. (c) represents diagrams proportional to gluon condensate with gluons lines attached to the light quarks only, (d) represents those where the gluons are attached to the heavy quarks only, while (e) represents those where one gluon is attached to the heavy quark and the other to a light quark in all possible ways. (f) and (g) represent all diagrams that contain the quark-gluon condensate.

where $\alpha, \beta, \dots, \alpha', \beta', \dots$ are Dirac spinor indices. After making the required contractions using the definition

$$iS_q^{\alpha\beta}(x) \equiv \langle 0|T[q_a^\alpha(x)\bar{q}_b^\beta(0)]|0\rangle \quad (3.32)$$

the Eq. (3.31) becomes

$$\begin{aligned} \Pi^{(a)}(q^2) &= -i \int d^4x e^{iq \cdot x} \epsilon^{abc} \epsilon^{a'b'c'} (C\gamma_\mu)^{\alpha\beta} (\gamma_5 \gamma^\mu)^{\delta\sigma} (i\gamma_5)^{\tau\theta} (\gamma^{\mu'} \gamma_5)^{\sigma'\delta'} (\gamma_{\mu'} C)^{\beta'\alpha'} \\ &\quad \times (i\gamma_5)^{\theta'\tau'} \left[iS_{u, ab'}^{\alpha\beta'}(x) iS_{u, ba'}^{\beta\alpha'}(x) iS_{d, cc'}^{\sigma\sigma'}(x) iS_{ch, d'd}^{\tau'\tau}(-x) iS_{d, dd'}^{\theta\theta'}(x) \right. \\ &\quad - iS_{u, ab'}^{\alpha\beta'}(x) iS_{u, ba'}^{\beta\alpha'}(x) iS_{d, cd'}^{\sigma\theta'}(x) iS_{ch, d'd}^{\tau'\tau}(-x) iS_{d, dc'}^{\theta\theta'}(x) \\ &\quad - iS_{u, aa'}^{\alpha\alpha'}(x) iS_{u, bb'}^{\beta\beta'}(x) iS_{d, cc'}^{\sigma\sigma'}(x) iS_{ch, d'd}^{\tau'\tau}(-x) iS_{d, dd'}^{\theta\theta'}(x) \\ &\quad \left. + iS_{u, aa'}^{\alpha\alpha'}(x) iS_{u, bb'}^{\beta\beta'}(x) iS_{d, cd'}^{\sigma\theta'}(x) iS_{ch, d'd}^{\tau'\tau}(-x) iS_{d, dc'}^{\theta\theta'}(x) \right] \\ &= -i \int d^4x e^{iq \cdot x} \epsilon^{abc} \epsilon^{a'b'c'} \left\{ Tr \left[iS_{u, ab'}(x) (\gamma_{\mu'} C) iS_{u, ba'}^T(x) (C\gamma_\mu) \right] \right. \\ &\quad \times Tr \left[iS_{d, dd'}(x) i\gamma_5 iS_{ch, d'd}(-x) i\gamma_5 \right] \gamma_5 \gamma^\mu iS_{d, cc'}(x) \gamma^{\mu'} \gamma_5 \\ &\quad - Tr \left[iS_{u, ab'}(x) (\gamma_{\mu'} C) iS_{u, ba'}^T(x) (C\gamma_\mu) \right] \\ &\quad \times \gamma_5 \gamma^\mu iS_{d, cd'}(x) i\gamma_5 iS_{ch, d'd}(-x) i\gamma_5 iS_{d, dc'}(x) \gamma^{\mu'} \gamma_5 \\ &\quad - Tr \left[iS_{u, bb'}(x) (\gamma_{\mu'} C) iS_{u, aa'}^T(x) (C\gamma_\mu) \right] \\ &\quad \times Tr \left[iS_{d, dd'}(x) i\gamma_5 iS_{ch, d'd}(-x) i\gamma_5 \right] \gamma_5 \gamma^\mu iS_{d, cc'}(x) \gamma^{\mu'} \gamma_5 \\ &\quad \left. + Tr \left[iS_{u, bb'}(x) (\gamma_{\mu'} C) iS_{u, aa'}^T(x) (C\gamma_\mu) \right] \right. \\ &\quad \left. \times \gamma_5 \gamma^\mu iS_{d, cd'}(x) i\gamma_5 iS_{ch, d'd}(-x) i\gamma_5 iS_{d, dc'}(x) \gamma^{\mu'} \gamma_5 \right\} \quad (3.33) \end{aligned}$$

For the perturbative part the propagators for light quarks and charm quark are

given as,

$$\begin{aligned}
iS_{q,ab}^{\alpha\beta}(x) &= \frac{i}{2\pi^2} \frac{\not{x}^{\alpha\beta}}{x^2} \delta_{ab} = iS_q^{\alpha\beta} \delta_{ab} \\
iS_{ch,ab}^{\alpha\beta}(x) &= \int \frac{d^4k}{(2\pi)^4} e^{-ik \cdot x} i \frac{(\not{k} + m_c)^{\alpha\beta}}{k^2 - m_c^2} \delta_{ab} = iS_{ch}^{\alpha\beta} \delta_{ab}
\end{aligned} \tag{3.34}$$

where q denotes up and down quarks and ch denotes charm quark. After inserting Eq. (3.34) in Eq. (3.33) the color factors of the right hand side of the Eq. (3.33) are calculated for the first, second, third and fourth term respectively as

$$\begin{aligned}
\epsilon^{abc} \epsilon^{a'b'c'} \delta_{ab'} \delta_{ba'} \delta_{cc'} \delta_{d'd} \delta_{dd'} &= 3\epsilon^{abc} \epsilon^{bac} = -18 \\
\epsilon^{abc} \epsilon^{a'b'c'} \delta_{ab'} \delta_{ba'} \delta_{cd'} \delta_{d'd} \delta_{dc'} &= \epsilon^{abc} \epsilon^{bac} = -6 \\
\epsilon^{abc} \epsilon^{a'b'c'} \delta_{aa'} \delta_{bb'} \delta_{cc'} \delta_{dd'} \delta_{d'd} &= 3\epsilon^{abc} \epsilon^{abc} = 18 \\
\epsilon^{abc} \epsilon^{a'b'c'} \delta_{aa'} \delta_{bb'} \delta_{cd'} \delta_{d'd} \delta_{dc'} &= \epsilon^{abc} \epsilon^{abc} = 6
\end{aligned} \tag{3.35}$$

Making use of these values of color factors the Eq. (3.33) becomes

$$\begin{aligned}
\Pi^{(a)}(q^2) &= i \int d^4x e^{iq \cdot x} \left\{ 36 \text{Tr} \left[iS_u(x) (\gamma_{\mu'} C) iS_u^T(x) (C \gamma_{\mu}) \right] \right. \\
&\quad \times \text{Tr} \left[iS_d(x) i\gamma_5 iS_{ch}(-x) i\gamma_5 \right] \gamma_5 \gamma^{\mu} iS_d(x) \gamma^{\mu'} \gamma_5 \\
&\quad - 12 \text{Tr} \left[iS_u(x) (\gamma_{\mu'} C) iS_u^T(x) (C \gamma_{\mu}) \right] \\
&\quad \left. \times \gamma_5 \gamma^{\mu} iS_d(x) i\gamma_5 iS_{ch}(-x) i\gamma_5 iS_d(x) \gamma^{\mu'} \gamma_5 \right\} .
\end{aligned} \tag{3.36}$$

After inserting $iS_q(x)$ and $iS_{ch}(x)$ into Eq. (3.36) and calculating the traces and contractions included in Eq. (3.36) the Eq. (3.36) becomes

$$\Pi^{(a)}(q^2) = i \int d^4x e^{iq \cdot x} \left\{ 33 \frac{(i)^7}{(2\pi^2)^4} \frac{4^3}{(x^2)^7} \int \frac{d^4k}{(2\pi)^4} e^{ik \cdot x} \not{x} \frac{k \cdot x}{k^2 - m_c^2} \right.$$

$$+96 \frac{(i)^7}{(2\pi^2)^4} \frac{1}{(x^2)^6} \int \frac{d^4 k}{(2\pi)^4} e^{ik \cdot x} \frac{m_c}{k^2 - m_c^2} \Big\} . \quad (3.37)$$

Using the equations given in App. D the result of the Eq. (3.37) can be obtained as

$$\begin{aligned} \Pi^{(a)}(q^2) = & \frac{-11}{5! 6! 2^{13} \pi^8} \int_0^1 du \frac{1}{(1-u)^5} \Big\{ \not{d} \Big[-36u(1-u)[-L(u)]^5 \\ & + 120q^2u^2(1-u)^2[-L(u)]^4 \Big] + m_c 72[-L(u)]^5 \Big\} \ln[-L] , \end{aligned} \quad (3.38)$$

whose imaginary part gives us

$$\begin{aligned} \frac{1}{\pi} \text{Im} \Pi^{(a)}(q^2) = & \frac{11}{5! 6! 2^{13} \pi^8} \int_0^\Lambda du \frac{1}{(1-u)^5} \Big\{ \not{d} \Big[-36u(1-u)[-L(u)]^5 \\ & + 120q^2u^2(1-u)^2[-L(u)]^4 \Big] + m_c 72[-L(u)]^5 \Big\} . \end{aligned} \quad (3.39)$$

Here the upper limit of the integrations is given by $\Lambda = 1 - m_c^2/q^2$ and $L(u) = q^2u(1-u) - m_c^2u$. A similar calculation is made for the Diagram (b) but for this part of the calculation the propagator for one of the light quark will take the form

$$iS_{q, ab}^{\alpha\beta}(x) = -\frac{1}{12} \langle \bar{q}q \rangle \delta_{ab} \delta^{\alpha\beta} . \quad (3.40)$$

Following the same steps followed for the calculation of the Diagram (a) the imaginary part of each diagram is calculated as

$$\begin{aligned} \frac{1}{\pi} \text{Im} \Pi^{(a)}(q^2) = & \frac{11}{5! 6! 2^{13} \pi^8} \int_0^\Lambda du \frac{1}{(1-u)^5} \Big\{ \not{d} \Big[-36u(1-u)[-L(u)]^5 \\ & + 120q^2u^2(1-u)^2[-L(u)]^4 \Big] + m_c 72[-L(u)]^5 \Big\} , \\ \frac{1}{\pi} \text{Im} \Pi^{(b)}(q^2) = & \frac{5 \langle \bar{q}q \rangle}{4! 4! 2^9 \pi^8} \int_0^\Lambda du \frac{1}{(1-u)^3} \Big\{ \not{d} 16m_c u [-L(u)]^3 \end{aligned}$$

$$\begin{aligned}
& + 8q^2 u(1-u)[-L(u)]^3 - [-L(u)]^4 \Big\} , \\
\frac{1}{\pi} \text{Im}\Pi^{(c)}(q^2) &= -\frac{11\langle\frac{\alpha_s}{\pi}G^2\rangle}{3\cdot 4!2^{14}\pi^6} \int_0^\Lambda du \frac{1}{(1-u)^3} \Big\{ \not{q}[-3u(1-u)[-L(u)]^3 \\
& + 6q^2 u^2(1-u)^2[-L(u)]^2 - \frac{8}{11}(1-u)[-L(u)]^3] \\
& + \frac{12}{11}m_c[-L(u)]^3 \Big\} , \\
\frac{1}{\pi} \text{Im}\Pi^{(d)}(q^2) &= \frac{11\langle\frac{\alpha_s}{\pi}G^2\rangle}{3!6!2^{12}\pi^6} \int_0^\Lambda du \frac{u^3}{(1-u)^5} \Big\{ \not{q}m_c^2[-3u(1-u)[-L(u)]^2 \\
& + 4q^2 u^2(1-u)^2[-L(u)]] + m_c[\frac{4}{11}[-L(u)]^3 \\
& + \frac{6}{11}q^2(1-u)^2[-L(u)]^2] \Big\} , \\
\frac{1}{\pi} \text{Im}\Pi^{(e)}(q^2) &= \frac{\langle\frac{\alpha_s}{\pi}G^2\rangle}{4!5!3\cdot 2^{10}\pi^6} \int_0^\Lambda du \frac{u}{(1-u)^4} \Big\{ \not{q}[(96u(1-u) \\
& + 5(1-u))[-L(u)]^3 - 192q^2 u^2(1-u)^2[-L(u)]^2] \\
& + 90m_c[-L(u)]^3 \Big\} , \\
\frac{1}{\pi} \text{Im}\Pi^{(f)}(q^2) &= \frac{5\langle\bar{q}g\sigma\cdot Gq\rangle}{3!3!2^{11}\pi^6} \int_0^\Lambda du \frac{1}{(1-u)^2} \Big\{ 12 \not{q}m_c u[-L(u)]^2 \\
& - [-L(u)]^3 + 6q^2 u(1-u)[-L(u)]^2 \Big\} , \\
\frac{1}{\pi} \text{Im}\Pi^{(g)}(q^2) &= \frac{\langle\bar{q}g\sigma\cdot Gq\rangle}{3!4!2^{10}\pi^6} \int_0^\Lambda du \frac{1}{(1-u)^3} \Big\{ \not{q}m_c[12u(1-u)[-L(u)]^2 \\
& - 60u^2[-L(u)]^2] - 12(1-u)[-L(u)]^3 \\
& + 72q^2 u(1-u)^2[-L(u)]^2 \\
& - \frac{u}{2}[-L(u)]^3 + 3q^2 u^2(1-u)[-L(u)]^2 \Big\} , \\
\frac{1}{\pi} \text{Im}\Pi^{(h)}(q^2) &= \frac{\langle\bar{q}q\rangle^2}{9\cdot 2^9\pi^4} \int_0^\Lambda du \frac{1}{(1-u)^2} \Big\{ \not{q}[12u(1-u)[-L(u)]^2 \\
& - 16q^2 u^2(1-u)^2[-L(u)] + 3(1-u)[-L(u)]^2]
\end{aligned}$$

$$\begin{aligned}
& +27m_c[-L(u)]^2 \Big\} , \\
\frac{1}{\pi}\text{Im}\Pi^{(i)}(q^2) &= \frac{5\langle\bar{q}q\rangle^3}{9\cdot 2^4\pi^2} \int_0^\Lambda du \left\{ -\not{q}m_c u + [-L(u)] - 2q^2 u(1-u) \right\} , \\
\frac{1}{\pi}\text{Im}\Pi^{(j)}(q^2) &= \frac{\langle\bar{q}q\rangle^4}{216} (-\not{q} + 22m_c) \delta(q^2 - m_c^2). \tag{3.41}
\end{aligned}$$

Our OPE calculation has been performed up to dimension 12 here. Up to dimension 5, we include all the gluonic contributions represented by the gluon condensate and the quark-gluon mixed condensate. Beyond the dimension 5, we include only tree-graph contributions which are expected to be important among higher dimensional operators. Other diagrams containing gluon components are expected to be suppressed by the small QCD coupling. Therefore, the higher order tree-graphs, which are the higher order quark condensates, will be able to give us an estimate on how big the typical higher order corrections should be beyond dimension 5. The integrations can be done analytically but we skip the lengthy and complicated analytic expressions. For the charm-quark propagators with two gluons attached, we use the momentum-space expressions given in Ref. [56]. The Wilson coefficients for light-quark condensates come from $\langle\bar{q}q\rangle^n$, where $n = 2, 3, 4$. This is in contrast with the OPE for Θ_{c2} , where the Wilson coefficient are non-zero only for $n = 4$.

The first important question to ask in the OPE is whether it is sensibly converging as an asymptotic expansion. For that, we choose to plot the Borel transformed OPE appearing in Eq. (3.14) after subtracting out the continuum contribution,

$$\Pi^{(j)}(M^2) = \int_0^\infty dq_0 \, e^{-q_0^2/M^2} [\rho_{\text{ope}}^{\pm,(j)}(q_0) - \rho_{\text{cont}}^{\pm,(j)}(q_0)] = 0. \quad (3.42)$$

Here $j = a, b, c..$ denotes each contribution in the OPE of the terms in Eq. (3.41) after adding according to the rules in Eq. (3.13).

We use the following QCD parameters in our sum rules [55, 42],

$$\begin{aligned} m_s &= 0.12 \text{ GeV} , \\ m_c &= 1.26 \text{ GeV} , \\ \left\langle \frac{\alpha_s}{\pi} G^2 \right\rangle &= (0.33 \text{ GeV})^4 , \\ \langle G^3 \rangle &= 0.045 \text{ GeV}^6 , \\ \langle \bar{q}q \rangle &= -(0.23 \text{ GeV})^3 , \\ \langle \bar{s}s \rangle &= 0.8 \langle \bar{q}q \rangle , \\ \langle \bar{q}g\sigma \cdot Gq \rangle &= (0.8 \text{ GeV}^2) \times \langle \bar{q}q \rangle , \\ \langle \bar{s}g\sigma \cdot Gs \rangle &= (0.8 \text{ GeV}^2) \times \langle \bar{s}s \rangle . \end{aligned} \quad (3.43)$$

Fig. (3.2) represents the OPE as defined in Eq. (3.42) with the imaginary part given in Eq. (3.41). One notes that for the negative parity case, the perturbative contribution is only a small fraction of the OPE, and hence do not converge.

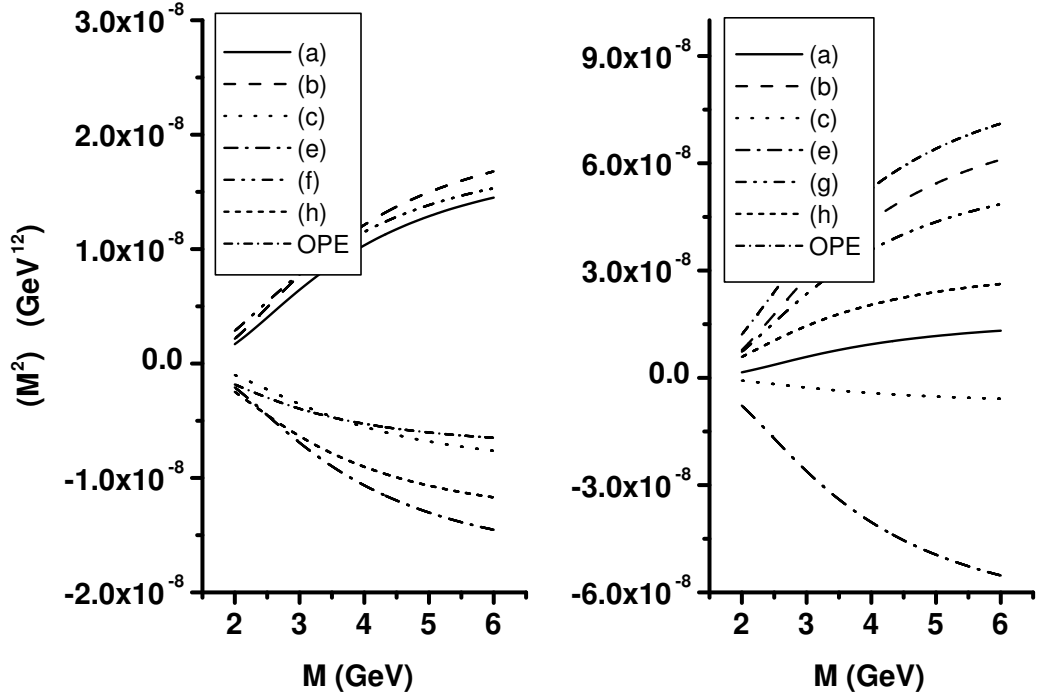


Figure 3.2: OPE as defined in Eq. (3.42) for the current Θ_{c1} and $S_0 = (3.3 \text{ GeV})^2$. The left (right) figure is for positive (negative) parity case. The solid line (a) represents the perturbative contribution. The line specified as OPE represents the sum of the power corrections only. (c) represents the gluon condensates. Other labels represent contribution from each term in Eq. (3.41). Here we plot only a few selected terms in the OPE.

For the positive parity case, the power corrections alternate in sign, and the gluon condensate, which represents the light diquark correlation, is only a small correction to the power correction. Hence, such structure, would hardly couple to a pentaquark state, and it is meaningless to perform a detailed QCD sum rule analysis. We present the result with the continuum threshold $s_0 = (3.3 \text{ GeV})^2$. This value is chosen in the range $\sqrt{s_0} = 3.2 - 3.6 \text{ GeV}$, which has been used to analyze the anticharmed-pentaquark sum rule in Ref [48]. However changing s_0 does not change the relative strength of each contribution, and hence the conclusion of this section. We will therefore, analyze the subsequent OPE with the same threshold.

3.4.2 The OPE for Θ_{c2}

The OPE for Θ_{c2} are given in Ref.[48]. Here, we rewrite the result for completeness,

$$\begin{aligned}
\frac{1}{\pi} \text{Im}\Pi^{(a)}(q^2) &= -\frac{1}{5 \cdot 5! \cdot 2^{12} \pi^8} \int_0^\Lambda du \frac{1}{(1-u)^5} \{ \not{q}(1-u) + m_c \} [-L(u)]^5, \\
\frac{1}{\pi} \text{Im}\Pi^{(b)}(q^2) &= -\frac{1}{3! \cdot 3! \cdot 2^{10} \pi^6} \left\langle \frac{\alpha_s}{\pi} G^2 \right\rangle \int_0^\Lambda du \frac{1}{(1-u)^3} \{ \not{q}(1-u) \\
&\quad + m_c \} [-L(u)]^3, \\
\frac{1}{\pi} \text{Im}\Pi^{(c)}(q^2) &= -\frac{1}{54} \langle \bar{q}q \rangle^4 (\not{q} + m_c) \delta(q^2 - m_c^2), \\
\frac{1}{\pi} \text{Im}\Pi^{(d)}(q^2) &= -\frac{1}{5! \cdot 3! \cdot 3 \cdot 2^{10} \pi^6} \left\langle \frac{\alpha_s}{\pi} G^2 \right\rangle \int_0^\Lambda du \frac{u^3}{(1-u)^5} \\
&\quad \times \left\{ 3m_c^2 \not{q}(1-u) + m_c(1-u)(3-5u)q^2 + 2um_c^3 \right\} [-L(u)]^2,
\end{aligned}$$

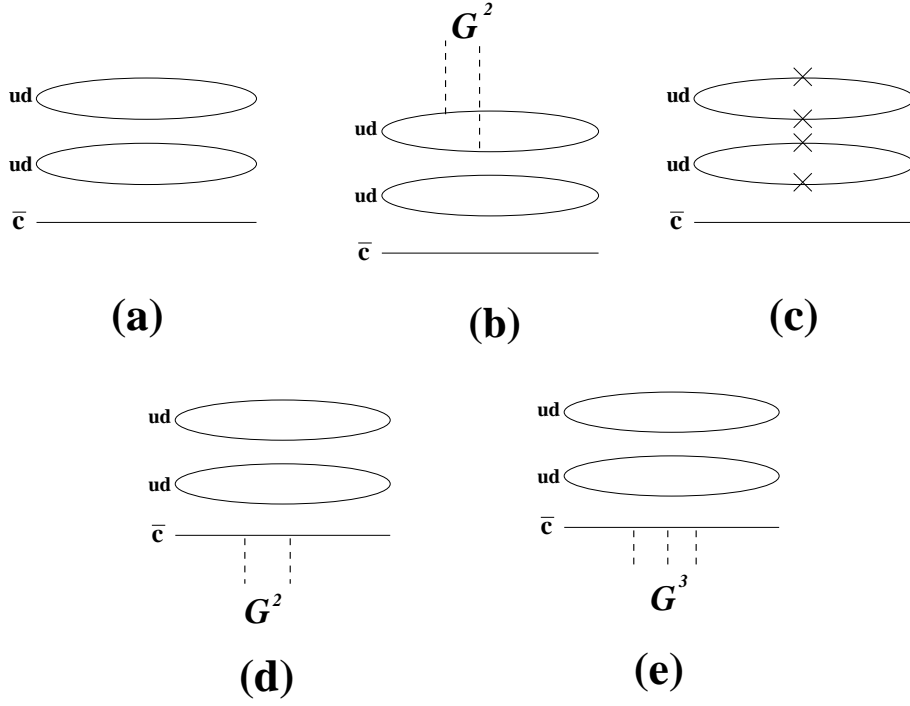


Figure 3.3: Schematic OPE diagrams for the current Θ_{c2} in Eq. (3.44). Each label corresponds to that in Eq. (3.44). All the other notations in this figure are the same as Fig. 3.1.

$$\begin{aligned}
\frac{1}{\pi} \text{Im}\Pi^{(e)}(q^2) &= -\frac{\langle G^3 \rangle}{5! 4! 2^{13} \pi^8} \int_0^\Lambda du \frac{u}{(1-u)} \left\{ \not{q} \left[q^2 \left(\frac{5u}{2} - 1 \right) (1-u) \right. \right. \\
&\quad \left. \left. - m_c^2 \left(\frac{3u}{2} + 7 \right) \right] + 6m_c q^2 (2u-1) \right. \\
&\quad \left. \left. - 2m_c^3 \frac{3u+1}{1-u} \right\} [-L(u)]. \tag{3.44}
\end{aligned}$$

The diagrams corresponding to every term above, denoted by the superscripts (a) – (e), is given in the Fig. 3.3 which can also be found in Ref. [48].

Fig. 3.4 represents the OPE as defined in Eq. (3.42) with the imaginary part in Eq. (3.44). As can be seen from the left figure, the OPE without the perturbative contribution is dominated by the gluon condensate coming from the light diquarks. This suggests that the diquark correlation is the dominant interaction among the quarks and heavy antiquark in the positive parity channel. Moreover, the perturbative contribution is larger than sum of the power corrections denoted as “OPE” in the figure. Therefore, the pentaquark could couple strongly to this current and a detailed QCD sum rule analysis is sensible. The situation changes for the negative channel, where the power corrections have alternating signs, and hence becomes less reliable.

3.4.3 The OPE for Θ_{cs1}

The OPE for this current is given as follows

$$\begin{aligned}
\frac{1}{\pi} \text{Im}\Pi^{(a)}(q^2) &= \frac{1}{5 \cdot 5! 2^{12} \pi^8} \int_0^\Lambda du \frac{1}{(1-u)^5} \{ \not{q}(u-1) - m_c \} [-L(u)]^5, \\
\frac{1}{\pi} \text{Im}\Pi^{(b)}(q^2) &= \frac{m_s(2\langle \bar{q}q \rangle + \langle \bar{s}s \rangle)}{3!3!2^8 \pi^6} \int_0^\Lambda du \frac{1}{(1-u)^3} \{ \not{q}(u-1) - m_c \} [-L(u)]^3,
\end{aligned}$$

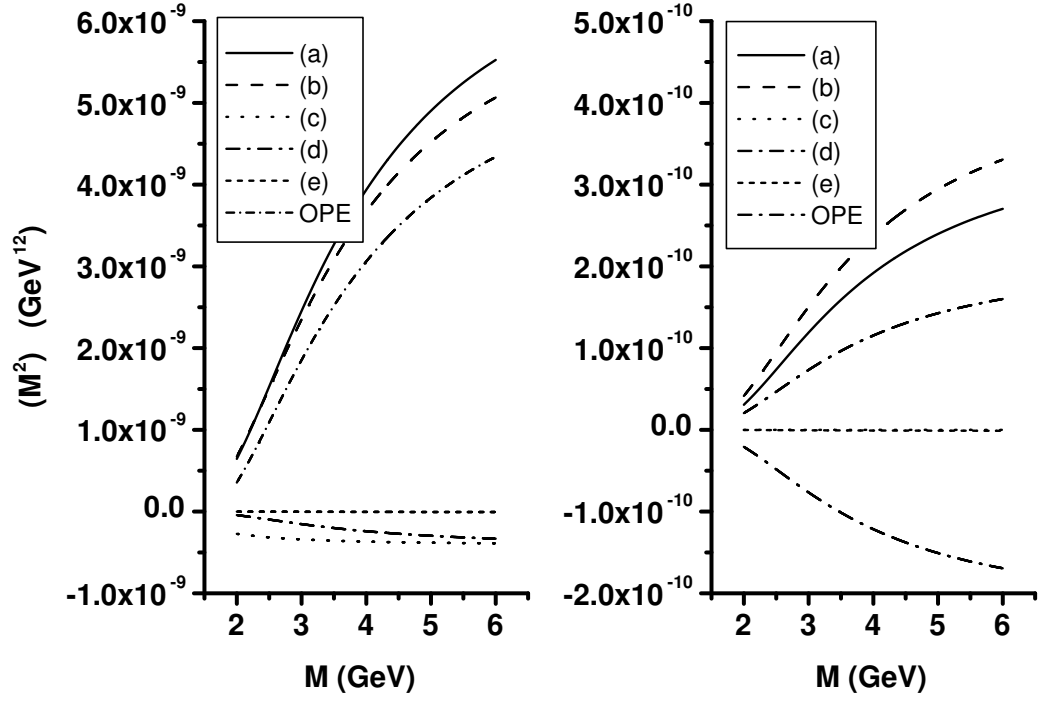


Figure 3.4: A similar figure as Fig. 3.2 for the current Θ_{c2} . Here each label represents contribution from each term in Eq. (3.44). The gluon condensates (b) are the dominant power correction in the positive parity channel (left figure).

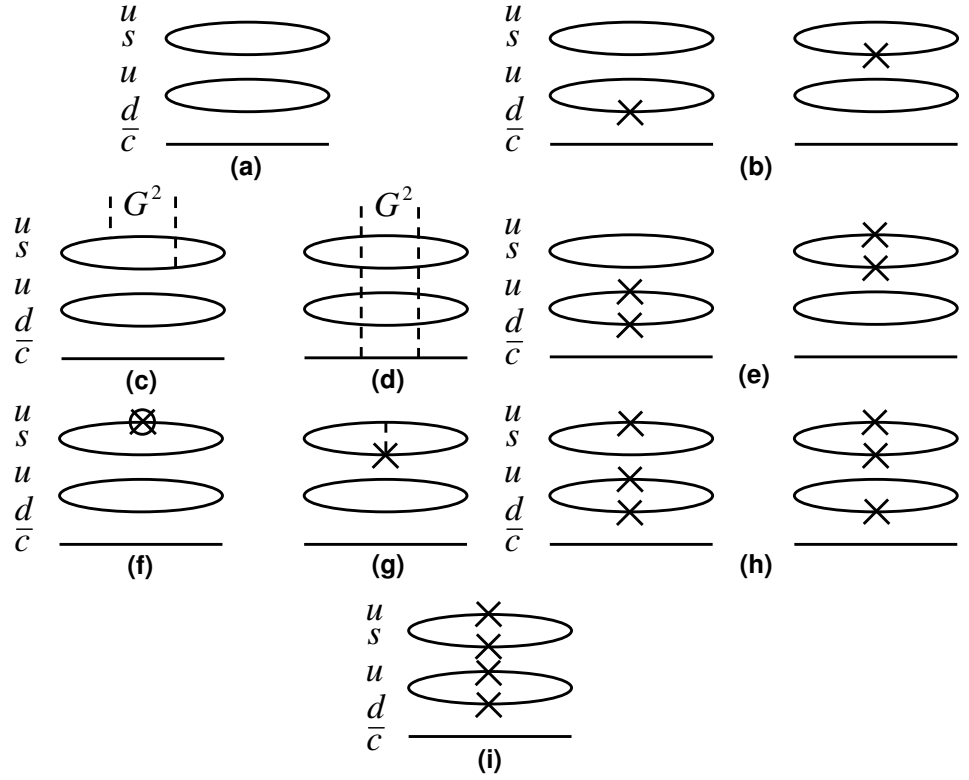


Figure 3.5: Schematic OPE diagrams for the currents Θ_{cs1} in Eq. (3.45) and Θ_{cs2} in Eq. (3.46). Each label corresponds to that in Eq. (3.45) or Eq. (3.46). All the other notations in this figure are the same as Fig. 3.1.

$$\begin{aligned}
\frac{1}{\pi} \text{Im}\Pi^{(c)}(q^2) &= \frac{\langle \frac{\alpha_s}{\pi} G^2 \rangle}{3!3!2^{10}\pi^6} \int_0^\Lambda du \frac{1}{(1-u)^3} \{ \not{d}(u-1) - m_c \} [-L(u)]^3, \\
\frac{1}{\pi} \text{Im}\Pi^{(d)}(q^2) &= -\frac{\langle \frac{\alpha_s}{\pi} G^2 \rangle}{3 \cdot 3!5!2^{10}\pi^6} \int_0^\Lambda du \frac{u^3}{(1-u)^5} \{ \not{d}3m_c^2(1-u) \\
&\quad + m_c(1-u)(3-5u)q^2 + 2um_c^3 \} [-L(u)]^2 \\
\frac{1}{\pi} \text{Im}\Pi^{(e)}(q^2) &= \frac{(\langle \bar{q}q \rangle^2 + \langle \bar{q}q \rangle \langle \bar{s}s \rangle)}{3 \cdot 2^7 \pi^4} \int_0^\Lambda du \frac{1}{(1-u)^2} \{ \not{d}(u-1) - m_c \} [-L(u)]^2, \\
\frac{1}{\pi} \text{Im}\Pi^{(f)}(q^2) &= \frac{m_s \langle \bar{q}D^2q \rangle}{2^{10}\pi^6} \int_0^\Lambda du \frac{1}{(1-u)^2} \{ \not{d}(u-1) - m_c \} [-L(u)]^2, \\
\frac{1}{\pi} \text{Im}\Pi^{(g)}(q^2) &= \frac{m_s \langle \bar{s}g\sigma \cdot Gs \rangle}{3 \cdot 2^{11}\pi^6} \int_0^\Lambda du \frac{1}{(1-u)^2} \{ \not{d}(u-1) - m_c \} [-L(u)]^2, \\
\frac{1}{\pi} \text{Im}\Pi^{(h)}(q^2) &= \frac{m_s(2\langle \bar{q}q \rangle^3 + \langle \bar{q}q \rangle^2 \langle \bar{s}s \rangle)}{9 \cdot 2^4 \pi^2} \int_0^\Lambda du \{ \not{d}(u-1) - m_c \}, \\
\frac{1}{\pi} \text{Im}\Pi^{(i)}(q^2) &= \frac{\langle \bar{q}q \rangle^3 \langle \bar{s}s \rangle}{54} (\not{d} + m_c) \delta(q^2 - m_c^2). \tag{3.45}
\end{aligned}$$

Note here again that the superscripts correspond to the diagrams shown in Fig. 3.5. The dimension-5 condensate involving D^2 is related to the quark-gluon condensate via $\langle \bar{q}D^2q \rangle = \langle \bar{q}g\sigma \cdot Gq \rangle/2$. Similar relation holds for the corresponding strange-quark condensate. The correction to this relation is proportional to square of the quark mass which should be very small even for the strange quark. Fig. 3.6 represents the OPE as defined in Eq. (3.42) with the imaginary part in Eq. (3.45). We have only included a few terms in the OPE to show how each term contributes differently to the sum rule. As can be seen from the figure, the line denoted as “OPE”, sum of the power corrections are much larger than the perturbative contribution. Moreover, the gluon condensate from diquarks is only a small fraction of the large higher order correction. This suggests that the OPE does not converge and it is very unlikely that the diquark correlation will remain

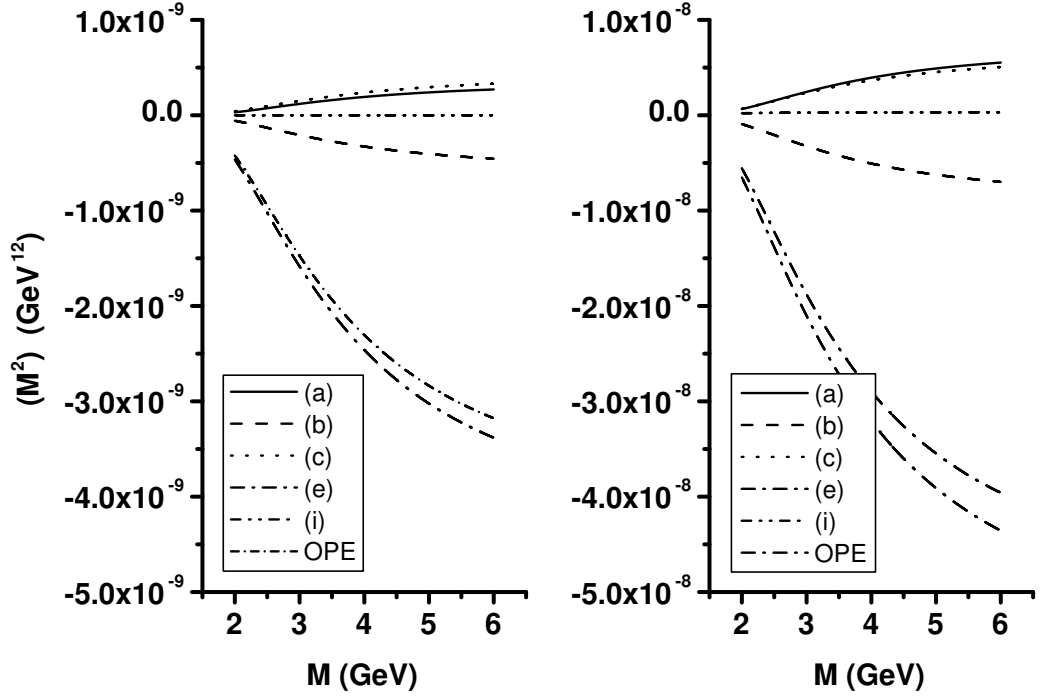


Figure 3.6: A similar figure as Fig. 3.2 for the current Θ_{cs1} with $S_0 = (3.3 \text{ GeV})^2$. Here each label represents contribution from each term in Eq. (3.45).

an important mechanism in this configuration.

3.4.4 The OPE for Θ_{cs2}

The OPE for this current is given as follows

$$\begin{aligned}
\frac{1}{\pi} \text{Im}\Pi^{(a)}(q^2) &= \frac{1}{5 \cdot 5! 2^{12} \pi^8} \int_0^\Lambda du \frac{1}{(1-u)^5} \{ \not{q}(u-1) - m_c \} [-L(u)]^5, \\
\frac{1}{\pi} \text{Im}\Pi^{(b)}(q^2) &= \frac{m_s(-2\langle \bar{q}q \rangle + \langle \bar{s}s \rangle)}{3!3!2^8 \pi^6} \int_0^\Lambda du \frac{1}{(1-u)^3} \{ \not{q}(u-1) - m_c \} [-L(u)]^3, \\
\frac{1}{\pi} \text{Im}\Pi^{(c)}(q^2) &= \frac{\langle \frac{\alpha_s}{\pi} G^2 \rangle}{3!3!2^{10} \pi^6} \int_0^\Lambda du \frac{1}{(1-u)^3} \{ \not{q}(u-1) - m_c \} [-L(u)]^3, \\
\frac{1}{\pi} \text{Im}\Pi^{(d)}(q^2) &= -\frac{\langle \frac{\alpha_s}{\pi} G^2 \rangle}{3 \cdot 3!5!2^{10} \pi^6} \int_0^\Lambda du \frac{u^3}{(1-u)^5} \{ \not{q} 3m_c^2(1-u)
\end{aligned}$$

$$\begin{aligned}
& + m_c(1-u)(3-5u)q^2 + 2um_c^3 \} [- L(u)]^2 \\
\frac{1}{\pi} \text{Im}\Pi^{(e)}(q^2) &= \frac{(\langle \bar{q}q \rangle^2 - \langle \bar{q}q \rangle \langle \bar{s}s \rangle)}{3 \cdot 2^7 \pi^4} \int_0^\Lambda du \frac{1}{(1-u)^2} \{ \not{q}(u-1) - m_c \} [- L(u)]^2 , \\
\frac{1}{\pi} \text{Im}\Pi^{(f)}(q^2) &= \frac{-m_s \langle \bar{q} D^2 q \rangle}{2^{10} \pi^6} \int_0^\Lambda du \frac{1}{(1-u)^2} \{ \not{q}(u-1) - m_c \} [- L(u)]^2 , \\
\frac{1}{\pi} \text{Im}\Pi^{(g)}(q^2) &= \frac{m_s \langle \bar{s} g \sigma \cdot G s \rangle}{3 \cdot 2^{11} \pi^6} \int_0^\Lambda du \frac{1}{(1-u)^2} \{ \not{q}(u-1) - m_c \} [- L(u)]^2 , \\
\frac{1}{\pi} \text{Im}\Pi^{(h)}(q^2) &= \frac{m_s (-2 \langle \bar{q}q \rangle^3 + \langle \bar{q}q \rangle^2 \langle \bar{s}s \rangle)}{9 \cdot 2^4 \pi^2} \int_0^\Lambda du \{ \not{q}(u-1) - m_c \} , \\
\frac{1}{\pi} \text{Im}\Pi^{(i)}(q^2) &= \frac{-\langle \bar{q}q \rangle^3 \langle \bar{s}s \rangle}{54} (\not{q} + m_c) \delta(q^2 - m_c^2). \tag{3.46}
\end{aligned}$$

Again note that the OPE diagram for each label is shown in Fig. 3.5. Fig. 3.7 represents the OPE as defined in Eq. (3.42) with the imaginary part given in Eq. (3.46). Again, we have only included a few terms in the OPE to show a general trend of each contribution. For the negative parity case, the OPE has large contributions with alternating signs. The situation is better for the positive parity case, but again, the power corrections alternate in signs.

From all the previous analysis on the OPE for the charmed pentaquark with and without strangeness, we find that the one without strangeness with diquark structure are most reliable, and are dominated by gluon condensate coming from diquark correlation. It is interesting to note that this result is consistent with the Skyrme model calculation which predicts a bound state of pentaquarks in the nonstrange sector [17]. In the following, we will perform a more detailed analysis with the stable structure well represented by the interpolating current Θ_{c2} .

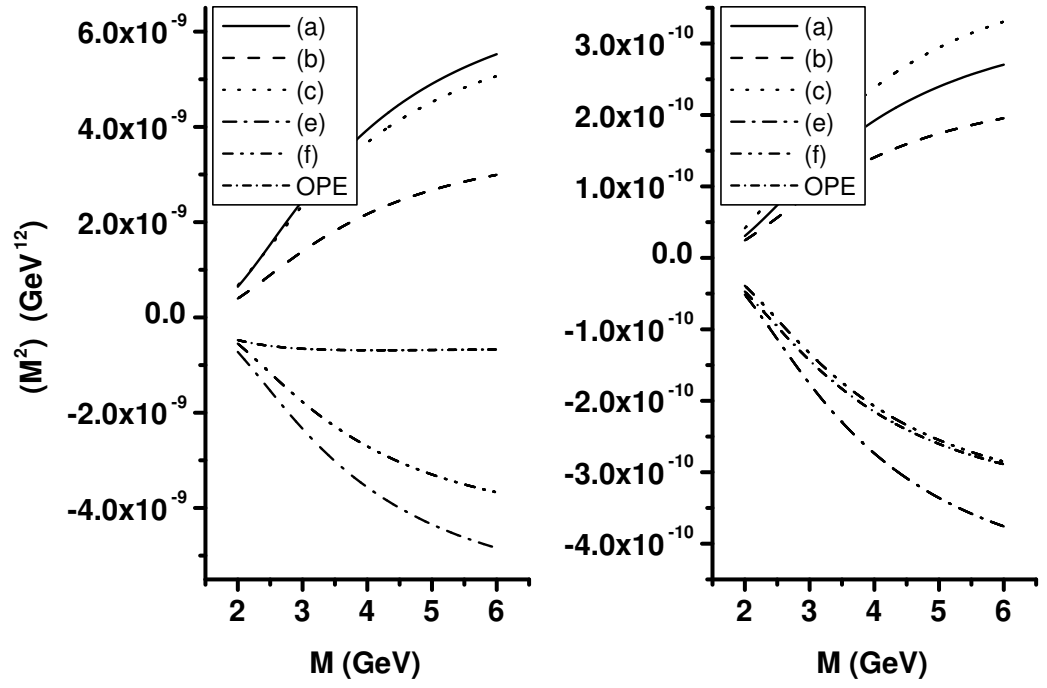


Figure 3.7: A similar figure as Fig. 3.2 for the current Θ_{cs2} with $S_0 = (3.3 \text{ GeV})^2$. Here each label represents each term in Eq. 3.46

CHAPTER 4

QCD SUM RULES AND ANALYSIS

4.1 The Couplings to the DN Continuum, λ_{DN}

As discussed before, it is important to subtract out the contribution from the DN continuum. For that, one needs to know the coupling strength λ_{DN} . Here we determine this for the currents without strange quarks, $\lambda_{DN,c2}$. In the case of Θ^+ (1540) [51], the soft-kaon theorem was used to convert the external kaon state, corresponding to the D meson states in Eq. (3.17) and Eq. (3.24), to a commutation relation of the operator and the corresponding axial charge. The strength of the resulting five-quark operator with an external nucleon state was then obtained from a separate nucleon sum rule analysis with the same five-quark nucleon current. However, applying the soft D meson limit will not work in the present case.

Instead, we determine the coupling strength directly from the sum rule method. To do that, we eliminate the contribution from the low-lying pole by introducing

the additional weight $W(q^2) = q^2 - m_\Theta^2$ in Eq. (3.7). We take $m_\Theta = 3$ GeV, and confirm that changing it by ± 200 MeV have less than 5 % effect on the λ_{DN} value. This way of eliminating a certain pole is sometimes used in QCD sum rules [76, 77]. Then, substituting the corresponding imaginary parts, we find,

$$|\lambda_{DN}|^2 = \frac{\int_{m_c^2}^{s_0} dq^2 e^{-q^2/M^2} (q^2 - m_\Theta^2) \frac{1}{\pi} \text{Im}\Pi_i^{\text{ope}}(q^2)}{\int_{(m_N+m_D)^2}^{s_0} dq^2 e^{-q^2/M^2} (q^2 - m_\Theta^2) \frac{1}{\pi} \text{Im}\Pi_i^{DN}(q^2)}, \quad (i = 1, q) \quad (4.1)$$

where the $i = 1, q$ in $\text{Im}\Pi$ represent the part proportional to 1 or \not{q} in the respective imaginary part, and $\text{Im}\Pi^{DN}$ is the spectral density in Eq. (3.22) or in Eq. (3.26) without the $|\lambda_{DN}|^2$ prefactor.

Fig. 4.1 shows the plot of Eq. (4.1). The two dotted (solid) lines represent boundary curves with the least Borel mass dependence for the λ_{DN} from the 1 (q) sum rules. λ_{DN} should not only be independent of the Borel mass but also independent of the sum rule from which it is obtained. However, the results coming from either $i = q$ or $i = 1$ sum rule differ slightly. Inspecting the OPE, one finds that the contributions from higher dimensional operators are consecutively suppressed for the $i = q$ sum rule, while that is not so for the $i = 1$ sum rule. Therefore, the value from the former sum rule should be more reliable. Nonetheless, to allow for all variations, we will choose the following range for the $|\lambda_{DN}|^2$ values,

$$2 \times 10^{-5} \text{GeV}^{10} < |\lambda_{DN,c2}|^2 < 3 \times 10^{-5} \text{GeV}^{10}. \quad (4.2)$$

Similar attempts to determine $\lambda_{DN,c1}$ give vastly different values from either $i = q$

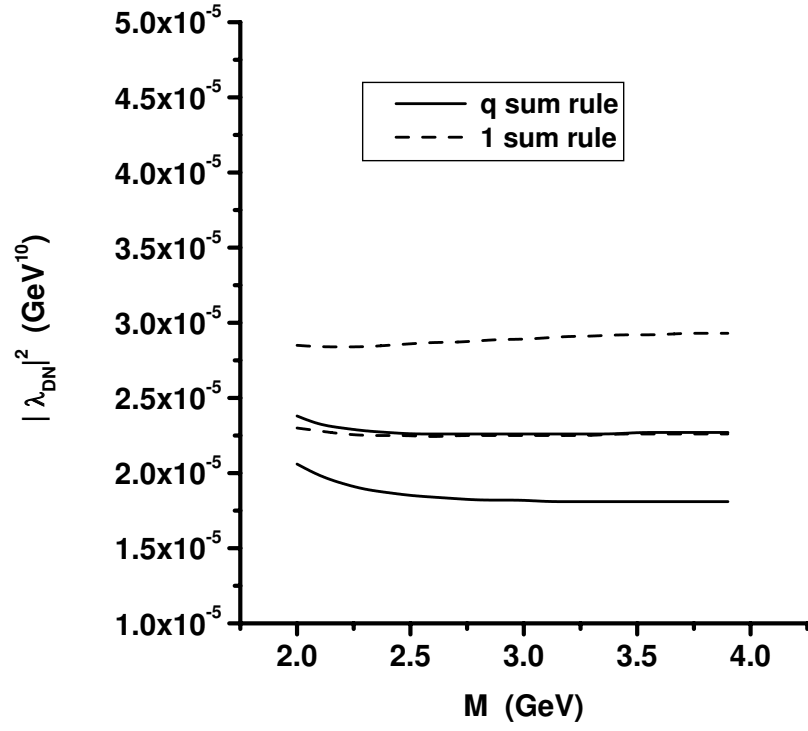


Figure 4.1: The $|\lambda_{DN,c2}|^2$ from the sum rule for $i = q$ (solid) line and $i = 1$ (dashed line). The upper (lower) solid or dashed lines in this case are for $S_0 = (3.8 \text{ GeV})^2$ [$S_0 = (3.7 \text{ GeV})^2$].

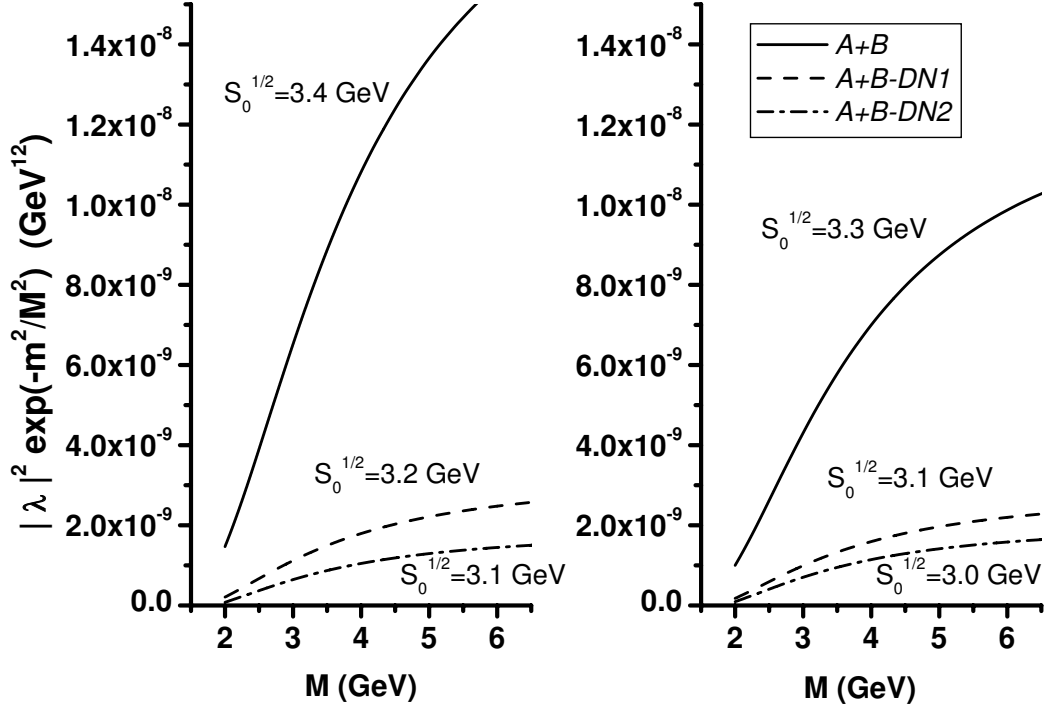


Figure 4.2: The left figure shows the left-hand side of Eq. (4.3) using Θ_{c2} for positive parity case with $|\lambda_{DN,c2}|^2 = 2 \times 10^{-5} \text{ GeV}^{10}$ (dashed line) and $|\lambda_{DN,c2}|^2 = 3 \times 10^{-5} \text{ GeV}^{10}$ (dot-dashed line). The solid line is when there is no DN continuum, $|\lambda_{DN,c2}|^2 = 0$. The right figure is obtained with different threshold parameters. See Eq. (3.12) for A and B .

or $i = 1$ sum rules. This reflects the non-convergence of OPE from which one can not expect a consistent result.

4.2 Parity

We will now concentrate on the sum rule obtained from Θ_{c2} . Using the dispersion relation in Eq. (3.14) and the spectral density in Eq. (3.27), one finds the

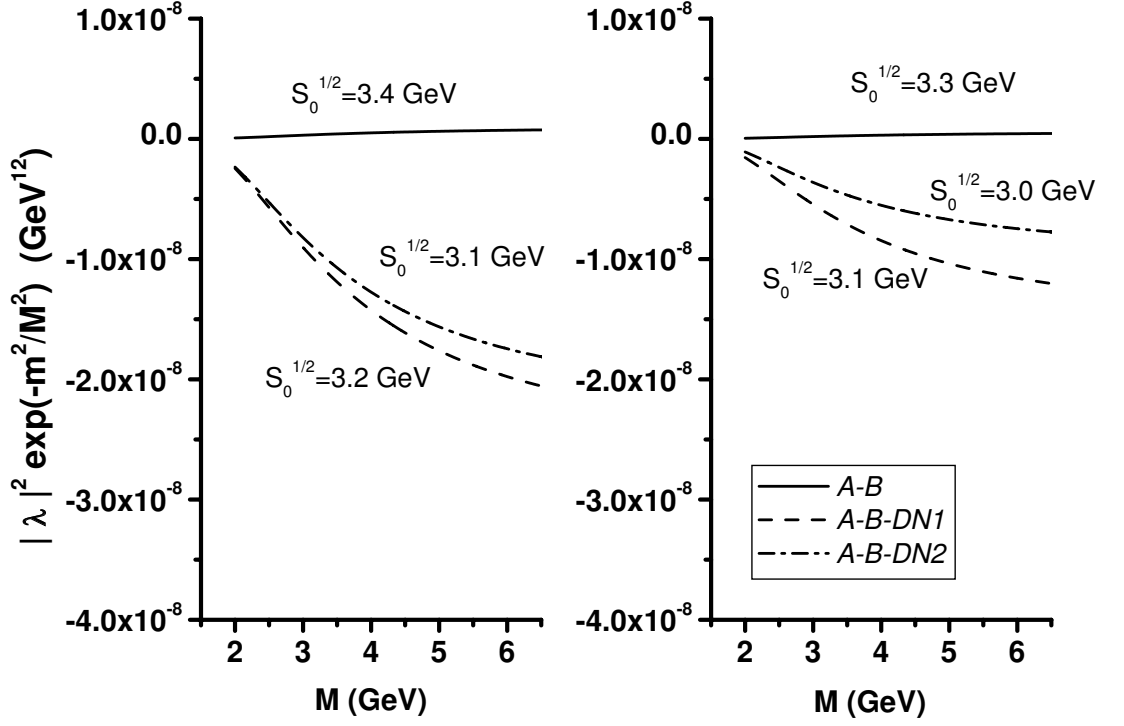


Figure 4.3: The left figure shows the left-hand side of Eq. (4.3) using Θ_{c2} for negative parity case with $|\lambda_{DN,c2}|^2 = 2 \times 10^{-5} \text{ GeV}^{10}$ (dashed line) and $|\lambda_{DN,c2}|^2 = 3 \times 10^{-5} \text{ GeV}^{10}$ (dot-dashed line). The solid line is when there is no DN continuum. The right figure is obtained with different threshold parameters.

following sum rule,

$$|\lambda_{\pm,c2}|^2 e^{-m_{\Theta_{\pm}}^2/M^2} = \int_0^{\sqrt{s_0}} dq_0 e^{-q_0^2/M^2} \left[\rho_{\text{ope}}^{\pm}(q_0) - \rho_{DN}^{\pm}(q_0) \right]. \quad (4.3)$$

As can be seen from Fig. 4.2, the left hand side of Eq. (4.3) is positive for positive parity case. For $|\lambda_{DN,c2}|^2 = 0$ (the solid lines), we have chosen the continuum threshold $s_0^{1/2}$ to be 3.4 GeV and 3.3 GeV, which gives the most stable pentaquark mass as we will show in the next subsection. Similar method was used to obtain the continuum thresholds when $|\lambda_{DN,c2}|^2 \neq 0$. However, Fig. 4.3 shows that the corresponding sum rule is negative for the negative parity case, suggesting that there can not be any negative parity state. This result also confirms the non-convergence of the OPE for the negative parity case, from which a consistent result can not be obtained. This can also be expected from the constituent quark picture. The two diquarks in Θ_{c2} current have opposite parities and, when they are combined with the antiquark, the configuration should be dominated by the positive-parity part in the nonrelativistic limit.

4.3 Mass

The sum rule for the Θ_c mass is obtained by taking the derivative of Eq. (4.3) with respect to $1/M^2$. The solid and dashed lines in Fig. 4.4 represent the mass for two different λ_{DN} values. The threshold parameters were obtained to give the most stable mass within the Borel window plotted. One notes that the inclusion

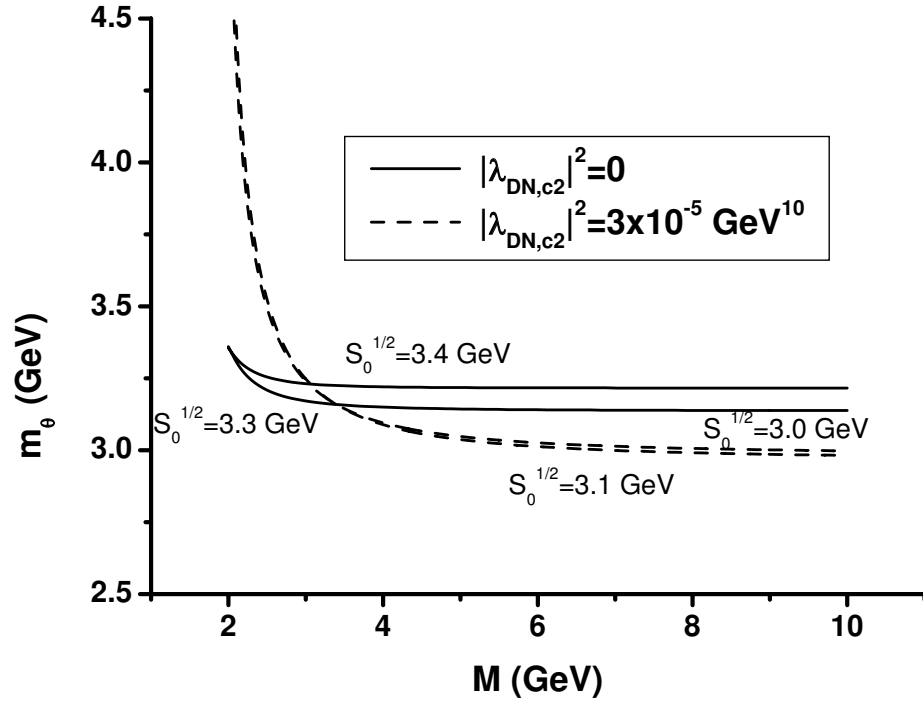


Figure 4.4: The mass obtained by taking the square root of the inverse ratio between left hand side of Eq. (4.3) and its derivative with respect to M^2 using Θ_{c2} .

of the coupling to the DN continuum states, reduces the mass to smaller values below 3 GeV. The curve with $\lambda_{DN,c2} = 2 \times 10^{-5} \text{ GeV}^{10}$ lies between the solid and dashed lines in Fig. 4.4. This suggests the possibility that the heavy pentaquark might actually be bound; namely, lies below the DN threshold. This is consistent with the constituent quark model picture, where one expects the diquark correlation to be more dominant than that of the quark-antiquark correlation as the participating antiquark becomes heavy. However, if this was the case, its existence can only be measured through its weak decay.

CHAPTER 5

CONCLUSIONS

In this thesis we have discussed one of the nonperturbative approaches, namely the QCD sum rules, and applied it to the heavy pentaquark Θ_c . In our analysis we have used pentaquark currents with and without strangeness with two different currents for each case. We have also included the DN two-particle irreducible contribution in our QCD sum rule calculation to refine the sum rules. To see whether the OPE calculations are convergent as an asymptotic expansion we have plotted the Borel transformed OPE, after subtracting out the continuum contribution, for each interpolating fields. From all the analysis on the OPE of the charmed pentaquark with and without strangeness we have found that the OPE is convergent only for the nonstrange pentaquark with a diquark structure. The OPE for this structure is dominated by the gluon condensate coming from the diquark, which nonperturbatively represents their strong correlation. By considering the result of the analysis on OPE we have performed a more detailed analysis with the stable structure well represented by the interpolating current Θ_{c2} . First of

all we have obtained the contribution coming from the DN continuum since it is important to subtract its contribution as discussed before. We have determined the coupling strength directly from the sum rule method and as a result we have chosen the range for the $|\lambda_{DN}|^2$ as $2 \times 10^{-5} \text{GeV}^{10} < |\lambda_{DN,c2}|^2 < 3 \times 10^{-5} \text{GeV}^{10}$. Then using the Eq. (4.3) the parity of the heavy pentaquark without strangeness has been obtained as positive, in agreement with the result reported earlier [48]. This can also be expected from the constituent quark picture where the two diquarks in Θ_{c2} currents have opposite parities and combined with an antiquark, and where the positive parity part should be dominant in the nonrelativistic limit. Taking the derivative of the Eq. (4.3) with respect to $\frac{1}{M^2}$ the sum rule for the mass of the Θ_c has been obtained. This analysis has shown that its mass lies below 3 GeV, when the DN irreducible contribution is explicitly included in the phenomenological side of the sum rule. The picture that we described here does not work so well in the light pentaquark Θ^+ , as the OPE are highly divergent [78] which can be seen in the picture of the OPE in the original sum rule paper for the light pentaquark state[42].

REFERENCES

- [1] LEPS Collaboration T. Nakano *et al.*, Phys. Rev. Lett. 91 (2003) 012002.
- [2] S. Stepanyan *et al.* (CLAS Collaboration), Phys. Rev. Lett. 91 (2003) 252001; J. Barth *et al.* (SAPHIR Collaboration), Phys. Lett. B 572 (2003) 127; V. V. Barmin *et al.* (DIANA Collaboration), Yad. Fiz. 66 (2003) 1763 [Phys. At. Nucl. 66 (2003) 1715]; V. Kubarovsky, S. Stepanyan (CLAS Collaboration), AIP Conf. Proc. 698 (2004) 543; A. E. Asratyan, A. G. Dolgolenko, M. A. Kubantsev, Yad. Fiz. **67** (2004) 704 [Phys. At. Nucl. **67** (2004) 682] V. Kubarovsky *et al.* (CLAS Collaboration), Phys. Rev. Lett. 92 (2004) 032001; A. Airapetian, et al. (HERMES Collaboration), Phys. Lett. B 585 (2004) 213; A. Aleev, et al. (SVD Collaboration), hep-ex/0401024. M. Abdel-Bary *et al.* (COSY-TOF Collaboration), Phys. Lett. B **595** (2004) 127 S. Chekanov *et al.* (ZEUS Collaboration), Phys. Lett. B **591** (2004) 7 Y. Oh, H. Kim and S. H. Lee, Phys. Rev. D **69**, 014009 (2004) Phys. Rev. D **69**, 094009 (2004) Phys. Rev. D **69**, 074016 (2004) Nucl. Phys. A **745**, 129 (2004) S. H. Lee, H. Kim and Y. Oh, J. Korean Phys. Soc. **46**, 774 (2005) Y. Oh and H. Kim, Phys. Rev. D **70**, 094022 (2004).
- [3] E. S. Smith, nucl-ex/0510078.
- [4] For a review on the present status of pentaquarks, see, K. H. Hicks, Prog. Part. Nucl. Phys. **55**, (2005) 647.
- [5] A. Aktas *et al.* (H1 Collaboration), Phys. Lett. B **588** (2004) 17.
- [6] D. O. Litvintsev (CDF Collaboration), Nucl. Phys. Proc. Suppl. **142**, (2005) 374.
- [7] U. Karshon (ZEUS Collaboration), hep-ex/0410029.
- [8] J. M. Link *et al.* (FOCUS Collaboration), Phys. Lett. B **622**, (2005) 229.
- [9] D. Diakonov, V. Petrov and M. V. Polyakov, Z. Phys. A **359**, (1997) 305.
- [10] T. D. Cohen, Phys. Lett. B **581**, (2004) 175.
- [11] C. Gignoux, B. Silvestre-Brac, J. M. Richard, Phys. Lett. B 193 (1987) 323.
- [12] H. J. Lipkin, Phys. Lett. B 195 (1987) 484.

- [13] S. Fleck, C. Gignoux, J. M. Richard and B. Silvestre-Brac, Phys. Lett. B 220 (1989) 616.
- [14] Fl. Stancu, Phys. Rev. D 58 (1998) 111501.
- [15] M. Genovese, J.-M. Richard, Fl. Stancu, S. Pepin, Phys. Lett. B 425 (1998) 171.
- [16] D. O. Riska, N. N. Scoccola, Phys. Lett. B 299 (1993) 338.
- [17] Y. Oh, B.-Y. Park, D.-P. Min, Phys. Lett. B 331 (1994) 362.
- [18] Y. Oh, B.-Y. Park, D.-P. Min, Phys. Rev. D 50 (1994) 3350.
- [19] Y. Oh, B.-Y. Park, Phys. Rev. D 51 (1995) 5016.
- [20] Y. S. Oh and B. Y. Park, Z. Phys. A **359**, (1997) 83.
- [21] K. Cheung, Phys. Rev. D **69** (2004) 094029.
- [22] T. E. Browder, I. R. Klebanov, D. R. Marlow, Phys. Lett. B **587** (2004) 62.
- [23] M. A. Nowak, M. Praszalowicz, M. Sadzikowski and J. Wasiluk, Phys. Rev. D **70** (2004) 031503.
- [24] H. Y. Cheng, C. K. Chua and C. W. Hwang, Phys. Rev. D **70** (2004) 034007.
- [25] M. E. Wessling, Phys. Lett. B **603** (2004) 152; **618** (2005) 269.
- [26] F. Stancu, Int. J. Mod. Phys. A **20** (2005) 1797.
- [27] K. Maltman, Int. J. Mod. Phys. A **20** (2005) 1977.
- [28] D. Pirjol and C. Schat, Phys. Rev. D **71**, (2005) 036004.
- [29] I. W. Stewart, M. E. Wessling and M. B. Wise, Phys. Lett. B **590**, 185 (2004).
- [30] R. L. Jaffe and F. Wilczek, Phys. Rev. Lett. **91** (2003) 232003.
- [31] M. Karliner and H. J. Lipkin, Phys. Lett. B **575** (2003) 249.
- [32] J. Hofmann and M. F. M. Lutz, Nucl. Phys. B **763** (2005) 90.
- [33] T. D. Cohen, P. M. Hohler and R. F. Lebed, Phys. Rev. D **72**, (2005) 074010.
- [34] R. L. Jaffe, Phys. Rev. Lett. **38**, (1977) 195; **38**, (1977) 617(E) .

- [35] E. Hiyama, M. Kamimura, A. Hosaka, H. Toki and M. Yahiro, hep-ph/0507105 [Phys. Lett. B (to be published)].
- [36] E. Hiyama, Y. Kino and M. Kamimura, Prog. Part. Nucl. Phys. **51** (2003) 223.
- [37] M. Kamimura, Prog. Theor. Phys. Suppl. **62** (1977) 236.
- [38] F. Stancu, AIP Conf. Proc. **775**, (2005) 32.
- [39] K. Maltman, Phys. Lett. B **604**, (2004) 175.
- [40] S. L. Zhu, Phys. Rev. Lett. **91** (2003) 232002.
- [41] R. D. Matheus, F. S. Navarra, M. Nielsen, R. Rodrigues da Silva, S. H. Lee, Phys. Lett. B **578** (2004) 323.
- [42] J. Sugiyama, T. Doi, M. Oka, Phys. Lett. B **581** (2004) 167.
- [43] M. Eidemuller, Phys. Lett. B **597** (2004) 314.
- [44] H. J. Lee, N. I. Kochelev and V. Vento, Phys. Lett. B **610** (2005) 50.
- [45] H. J. Lee, N. I. Kochelev and V. Vento, Phys. Rev. D **73** (2006) 014010.
- [46] M. Eidemuller, F. S. Navarra, M. Nielsen and R. Rodrigues da Silva, Phys. Rev. D. **72** (2005) 034003.
- [47] R. D. Matheus, F. S. Navarra, M. Nielsen and R. R. da Silva, Phys. Lett. B **602** (2004) 185.
- [48] H. Kim, S. H. Lee and Y. Oh, Phys. Lett. B **595** (2004) 293.
- [49] H. Kim and Y. Oh, Phys. Rev. D **72** (2005) 074012; M. E. Bracco, A. Lozea, R. D. Matheus, F. S. Navarra and M. Nielsen, Phys. Lett. B **624**, (2005) 217.
- [50] Y. Kondo, O. Morimatsu and T. Nishikawa, Phys. Lett. B **611** (2005) 93.
- [51] S. H. Lee, H. Kim and Y. Kwon, Phys. Lett. B **609** (2005) 252.
- [52] Y. Kwon, A. Hosaka and S. H. Lee, hep-ph/0505040.
- [53] S. Sasaki, Phys. Rev. Lett. **93** (2004) 152001.
- [54] F. Csikor, Z. Fodor, S. D. Katz, T. G. Kovacs, J. High Energy Phys. **11** (2003) 070.

- [55] M. A. Shifman, A. I. Vainshtein, and V. I. Zakharov, Nucl. Phys. B **147** (1979) 385; B **147** (1979) 448 ; B **147** (1979) 519.
- [56] L. J. Reinders, H. Rubinstein, and S. Yazaki, Phys. Rept. **127** (1985) 1.
- [57] L. J. Reinders, Acta Physica Polonica B **15** (1984) 329.
- [58] D. K. Griegel, Ph. D. Thesis, University of Maryland (1991).
- [59] T. Doi, Ph. D. Thesis, Tokyo Institute of Technology (2004).
- [60] X. Jin, Ph. D. Thesis, University of Maryland (1993).
- [61] T. D. Cohen, R. J. Furnstahl, D. K. Griegel, X. Jin, and S. Yazaki, Prog. Part. Nucl. Phys. **35** (1995) 221.
- [62] P. Colangelo, and A. Khodjamirian, hep-ph/0010175 v1.
- [63] K. Wilson, Phys. Rev. **179** (1969) 1499.
- [64] R. Tarrach, Nucl. Phys. B **196** (1982) 45.
- [65] J. Gasser, and H. Leutwyler, Phys. Rep. **87** (1982) 77.
- [66] V. M. Belyaev, and B. L. Ioffe, Zh. Eksp. Teor. Fiz. **83** (1982) 876; **84** (1983) 1236 [Sov. Phys. JETP **56** (1982) 493; **57** (1983) 716] .
- [67] D. B. Leinweber, Annals of Physics **198** (1990) 203.
- [68] A. I. Vainshtein, V. I. Zakharov, and M. A. Shifman, Pis'ma Zh. Eksp. Teor. Fiz. **27** (1978) 60 [JETP Lett. **27** (1978) 55] .
- [69] E. V. Shuryak, *The QCD Vacuum, Hadrons, and the Superdense Matter* (World Scientific, Singapore, 1988), and references there in.
- [70] A. A. Ovchinnikov, and A. A. Pivovarov, Yad. Fiz. **48** (1988) 1135 [Sov. J. Nucl. Phys. **48** (1988) 721] .
- [71] M. Kremer, and G. Schierholz, Phys. Lett. B **194** (1987) 283.
- [72] A. P. Bakulev, and A. V. Radyushkin, Phys. Lett. B **271** (1991) 223.
- [73] X. Jin, T. D. Cohen, R. J. Furnstahl, and D. K. Griegel, Phys. Rev. C **47** (1993) 2882.
- [74] D. Jido, N. Kodama, M. Oka, Phys. Rev. D **54** (1996) 4532.
- [75] X. M. Jin, J. Tang, Phys. Rev. D **56** (1997) 515.

- [76] X. M. Jin, Phys. Rev. D **55**, (1997) 1693.
- [77] H. Kim and M. Oka, Nucl. Phys. A **720**,(2003) 368.
- [78] R.D.Matheus, S.Narison, hep-ph/0412063.

APPENDIX A

NOTATIONS

In this Appendix some notations related to this thesis are given.

$$D_\mu = \partial_\mu - ig_s A_\mu^a t^a, \quad (\text{A.1})$$

$$[t^a, t^b] = if_{abc} t^c \quad (\text{A.2})$$

($t^a = \frac{\lambda_a}{2}$, where λ_a are the standard Gell-Mann matrices)

$$\begin{aligned} G_{\mu\nu}^a &= \frac{i}{g_s} [D_\mu, D_\nu]^a \\ &= \partial_\mu A_\nu^a - \partial_\nu A_\mu^a + g_s f^{abc} A_\mu^b A_\nu^c, \end{aligned} \quad (\text{A.3})$$

$$iS_q^{\alpha\beta}(x) \equiv \langle 0 | T [q_a^\alpha(x) \bar{q}_b^\beta(0)] | 0 \rangle \quad (\text{A.4})$$

(a, b : color indices, α, β : Dirac spinor indices)

Minkowski

Euclidean

$$g_{\mu\nu} = \text{diag}(+1, -1, -1, -1) \leftrightarrow \delta_{\mu\nu} = \text{diag}(+1, +1, +1, +1)$$

$$\begin{aligned}
\epsilon_M^{0123} = -\epsilon_{0123}^M = +1 & \leftrightarrow \epsilon_E^{0123} = \epsilon_{0123}^E = +1 \\
(x_M^0, x_M^i) & \leftrightarrow (ix_E^4, x_E^i) \quad (i = 1, 2, 3) \\
(P_M^0, P_M^i) & \leftrightarrow (iP_E^4, P_E^i) \\
(\gamma_M^0, \gamma_M^i) & \leftrightarrow (\gamma_E^4, \gamma_E^i) \\
\gamma_5^M = i\gamma_M^0\gamma_M^1\gamma_M^2\gamma_M^3 & \leftrightarrow \gamma_5^E = i\gamma_E^4\gamma_E^1\gamma_E^2\gamma_E^3 \\
\sigma_{\mu\nu}^M = \frac{i}{2}[\gamma_\mu^M, \gamma_\nu^M] & \leftrightarrow \sigma_{\mu\nu}^E = \frac{1}{2i}[\gamma_\mu^E, \gamma_\nu^E] .
\end{aligned} \tag{A.5}$$

APPENDIX B

GAMMA MATRIX ALGEBRA

In this Appendix the useful equations related to the algebras of Dirac gamma matrices are given.

$$\{\gamma_\mu, \gamma_\nu\} = \gamma_\mu \gamma_\nu + \gamma_\nu \gamma_\mu = 2g_{\mu\nu} . \quad (\text{B.1})$$

$$\gamma_5 = \gamma^5 = i\gamma^0 \gamma^1 \gamma^2 \gamma^3 . \quad (\text{B.2})$$

$$\{\gamma_5, \gamma_\nu\} = 0 . \quad (\text{B.3})$$

$$C \equiv i\gamma^2 \gamma^0 \quad (\text{charge conjugation matrix}) . \quad (\text{B.4})$$

$$C = -C^\dagger = -C^T = -C^{-1} , \quad C^2 = -1 . \quad (\text{B.5})$$

$$C\Gamma^T C = +\Gamma \quad \text{for} \quad \Gamma = \gamma_\mu, \sigma_{\mu\nu}, \gamma_5 \sigma_{\mu\nu} . \quad (\text{B.6})$$

$$C\Gamma^T C = -\Gamma \quad \text{for} \quad \Gamma = \gamma_5, \gamma_5 \gamma_\mu, (\not{x} \sigma_{\mu\nu} + \sigma_{\mu\nu} \not{x}) . \quad (\text{B.7})$$

$$\begin{aligned}
\gamma^\mu \gamma_\mu &= 4 , \\
\gamma^\mu \gamma_\nu \gamma_\mu &= -2\gamma_\nu , \\
\gamma^\mu \gamma_\alpha \gamma_\beta \gamma_\mu &= 4g_{\alpha\beta} , \\
\gamma^\mu \gamma_\alpha \gamma_\beta \gamma_\gamma \gamma_\mu &= -2\gamma_\gamma \gamma_\beta \gamma_\alpha , \\
\gamma^\mu \gamma_\alpha \gamma_\beta \gamma_\gamma \gamma_\lambda \gamma_\mu &= 2(\gamma_\lambda \gamma_\alpha \gamma_\beta \gamma_\gamma + \gamma_\gamma \gamma_\beta \gamma_\alpha \gamma_\lambda) , \\
\gamma^\mu \sigma_{\alpha\beta} \gamma_\mu &= 0 .
\end{aligned} \tag{B.8}$$

$$\begin{aligned}
\gamma^\alpha \sigma^{\mu\nu} &= \sigma^{\mu\nu} \gamma^\alpha + 2ig^{\alpha\mu} \gamma^\nu - 2ig^{\alpha\nu} \gamma^\mu , \\
\sigma^{\mu\nu} \gamma^\alpha &= \gamma^\alpha \sigma^{\mu\nu} + 2ig^{\nu\alpha} \gamma^\mu - 2ig^{\mu\alpha} \gamma^\nu .
\end{aligned} \tag{B.9}$$

$$\begin{aligned}
\sigma^{\alpha\beta} \sigma_{\alpha\beta} &= 12 , \\
\sigma^{\alpha\beta} \gamma^\mu \gamma^\nu \sigma_{\alpha\beta} &= 4\gamma^\nu \gamma^\mu + 8g^{\mu\nu} = 16g^{\mu\nu} - 4\gamma^\mu \gamma^\nu , \\
\sigma^{\alpha\beta} (\text{odd } \# \text{ of } \gamma \text{ matrices}) \sigma_{\alpha\beta} &= 0 .
\end{aligned} \tag{B.10}$$

$$\gamma_\mu \sigma_{\alpha\beta} = i(g_{\mu\alpha} \gamma_\beta - g_{\mu\beta} \gamma_\alpha) - \epsilon_{\mu\alpha\beta\lambda} \gamma^\lambda \gamma_5 \quad \text{or}, \tag{B.11}$$

$$\epsilon_{\mu\nu\lambda\omega} \gamma^\omega = -i\gamma_5 (g_{\mu\nu} \gamma_\lambda - g_{\mu\lambda} \gamma_\nu + g_{\nu\lambda} \gamma_\mu - \gamma_\mu \gamma_\nu \gamma_\lambda) \quad \text{or}, \tag{B.12}$$

$$\epsilon_{\mu\nu\alpha\beta} \gamma^\alpha \gamma^\omega \gamma^\beta = -2i\gamma_5 (\delta_\mu^\omega \gamma_\nu - \delta_\nu^\omega \gamma_\mu) . \tag{B.13}$$

$$\not{x} \sigma_{\mu\nu} + \sigma_{\mu\nu} \not{x} = -2\epsilon^{\mu\nu\alpha\beta} \gamma_5 \gamma_\alpha \cdot x_\beta . \tag{B.14}$$

$$\sigma_{\mu\nu} = \frac{i}{2} \epsilon^{\mu\nu\alpha\beta} \gamma_5 \sigma_{\alpha\beta} \Leftrightarrow \gamma_5 \sigma_{\mu\nu} = \frac{i}{2} \epsilon^{\mu\nu\alpha\beta} \sigma_{\alpha\beta} . \tag{B.15}$$

$$\gamma^\mu (\not{x}\sigma_{\mu\nu} + \sigma_{\mu\nu} \not{x})\gamma^\nu = -12i \not{x} . \quad (\text{B.16})$$

$$\epsilon_{\mu\nu\alpha\beta} \cdot \gamma^\mu (\not{x}\sigma^{\alpha\beta} + \sigma^{\alpha\beta} \not{x})\gamma^\nu = 0 . \quad (\text{B.17})$$

$$\text{Tr}[I] = 4 ,$$

$$\text{Tr}[\gamma_\mu] = 0 ,$$

$$\text{Tr}[\gamma_5] = 0 . \quad (\text{B.18})$$

The trace of an odd product of γ_μ matrices vanishes

$$\text{Tr}[\gamma_\mu\gamma_\nu] = 4g_{\mu\nu} ,$$

$$\text{Tr}[\sigma_{\mu\nu}] = 0 ,$$

$$\text{Tr}[\gamma_\mu\gamma_\nu\gamma_5] = 0 ,$$

$$\text{Tr}[\gamma_\mu\gamma_\nu\gamma_\rho\gamma_\sigma] = (4g_{\mu\nu}g_{\rho\sigma} - g_{\mu\rho}g_{\nu\sigma} + g_{\mu\sigma}g_{\nu\rho} ,$$

$$\text{Tr}[i\gamma_5\gamma_\mu\gamma_\nu\gamma_\eta\gamma_\delta] = 4\epsilon_{\mu\nu\eta\delta} \quad (\epsilon_{0123} = -1) ,$$

$$\text{Tr}[\gamma_\mu\gamma_\nu\gamma_\rho\gamma_\sigma\cdots] = \text{Tr}[\cdots\gamma_\sigma\gamma_\rho\gamma_\nu\gamma_\mu] . \quad (\text{B.19})$$

APPENDIX C

TRACES AND CONTRACTIONS

$$Tr[\not{x}\gamma_{\mu'} \not{x}\gamma_{\mu}] = 4(2x_{\mu'}x_{\mu} - x^2g_{\mu'\mu}) . \quad (C.1)$$

$$Tr[\gamma_5(\not{k} + m_c)\gamma_5] = 4m_c . \quad (C.2)$$

$$Tr[\not{x}\gamma_5(\not{k} + m_c)\gamma_5] = -4x \cdot k . \quad (C.3)$$

$$Tr[\not{x}\sigma_{\alpha\beta} + \sigma_{\alpha\beta} \not{x}] = 0 . \quad (C.4)$$

$$Tr[\not{x}\gamma_5\sigma_{\alpha\beta}(\not{k} + m_c)\gamma_5] = 4i(x_{\beta}k_{\alpha} - x_{\alpha}k_{\beta}) . \quad (C.5)$$

$$Tr[\not{x}\gamma_5(\not{k} + m_c)\sigma_{\alpha\beta}\gamma_5] = -4i(x_{\beta}k_{\alpha} - x_{\alpha}k_{\beta}) . \quad (C.6)$$

$$\begin{aligned} Tr[(\not{x}\sigma_{\alpha\beta} + \sigma_{\alpha\beta} \not{x})\gamma_{\mu'} \not{x}\gamma_{\mu}] &= -8i(x^2g_{\mu}^{\alpha}g_{\mu'}^{\beta} - x^2g_{\mu'}^{\alpha}g_{\mu}^{\beta} - x^{\alpha}x_{\mu}g_{\mu'}^{\beta} \\ &\quad + x^{\beta}x_{\mu}g_{\mu'}^{\alpha} + x^{\alpha}x_{\mu'}g_{\mu}^{\beta} - x^{\beta}x_{\mu'}g_{\mu}^{\alpha}) . \end{aligned} \quad (C.7)$$

$$\gamma^\alpha \sigma_{\alpha\beta} = 3i\gamma_\beta . \quad (\text{C.8})$$

$$\gamma^\beta \sigma_{\alpha\beta} \gamma^\alpha = -12i . \quad (\text{C.9})$$

$$\gamma^\alpha \not{x} \sigma_{\alpha\beta} = -i \not{x} \gamma_\beta - i2x_\beta . \quad (\text{C.10})$$

$$\sigma^{\alpha\beta} \not{x} \sigma_{\alpha\beta} = 0 . \quad (\text{C.11})$$

$$\sigma_{\alpha\beta}(\not{k} + m_c) \not{x} \gamma^\beta = i(2\gamma_\alpha k \cdot x - m_c \gamma_\alpha \not{x} + \not{x} \not{k} \gamma_\alpha - 2m_c x_\alpha) . \quad (\text{C.12})$$

$$\gamma^\alpha \sigma_{\alpha\beta}(\not{k} + m_c) \not{x} \gamma^\beta = 3i(4k \cdot x - 2m_c \not{x}) . \quad (\text{C.13})$$

$$\sigma_{\alpha\beta}(\not{k} + m_c) \sigma^{\alpha\beta} = 12m_c . \quad (\text{C.14})$$

$$\sigma_{\alpha\beta}(\not{k} + m_c) \not{x} \sigma^{\alpha\beta} = 4 \not{x} \not{k} + 8k \cdot x . \quad (\text{C.15})$$

$$\sigma_{\alpha\beta} \not{x} \not{k} \sigma^{\alpha\beta} = 4 \not{k} \not{x} + 8k \cdot x . \quad (\text{C.16})$$

$$\gamma^\alpha \not{x}(\not{k} + m_c) \sigma_{\alpha\beta} = i[(2k \cdot x - m_c \not{x})\gamma_\beta + \gamma_\beta \not{k} \not{x} - 2m_c x_\beta] . \quad (\text{C.17})$$

$$\gamma^\alpha \sigma_{\alpha\beta}(\not{k} + m_c) \gamma_\beta = -6i(\not{k} - 2m_c) . \quad (\text{C.18})$$

$$\gamma^\alpha(\not{k} + m_c) \sigma_{\alpha\beta} = i(-\not{k} \gamma_\beta + 2m_c \gamma_\beta - 2k_\beta + m_c \gamma_\beta) . \quad (\text{C.19})$$

$$\gamma^\alpha(\not{k} + m_c)\gamma_\alpha = -2 \not{k} + 4m_c . \quad (\text{C.20})$$

$$\gamma^\alpha \not{x}(\not{k} + m_c)\gamma_\alpha = 4k \cdot x - 2 \not{x}m_c . \quad (\text{C.21})$$

$$\gamma^\alpha \not{x}(\not{k} + m_c) \not{x}\gamma_\alpha = -2 \not{x} \not{k} \not{x} + 4x^2m_c . \quad (\text{C.22})$$

$$\gamma^\alpha \not{x}\sigma_{\alpha\beta}(\not{k} + m_c) \not{x}\gamma_\beta = -4i \not{x}k \cdot x - 2ix^2 \not{k} . \quad (\text{C.23})$$

APPENDIX D

USEFUL INTEGRALS AND EQUATIONS

Feynman parameters:

$$\frac{1}{A_1 A_2 \dots A_n} = \int_0^1 dx_1 \dots dx_n \delta(\sum x_i - 1) \frac{(n-1)!}{[x_1 A_1 + x_2 A_2 + \dots x_n A_n]^n} \quad (\text{D.1})$$

A more general form of the Feynman parameters is

$$\frac{1}{A_1^{m_1} A_2^{m_2} \dots A_n^{m_n}} = \int_0^1 dx_1 \dots dx_n \delta(\sum x_i - 1) \frac{\prod x_i^{m_i-1}}{[\sum x_i A_i]^{\sum m_i}} \frac{\Gamma(m_1 + \dots + m_n)}{\Gamma(m_1) \dots \Gamma(m_n)} \quad (\text{D.2})$$

The d dimensional integrals in Minkowski space:

$$\begin{aligned} \int \frac{d^d \ell}{(2\pi)^d} \frac{1}{(\ell^2 - \Delta)^n} &= \frac{(-1)^n i}{(4\pi)^{\frac{d}{2}}} \frac{\Gamma(n - \frac{d}{2})}{\Gamma(n)} \left(\frac{1}{\Delta}\right)^{n - \frac{d}{2}}, \\ \int \frac{d^d \ell}{(2\pi)^d} \frac{\ell^2}{(\ell^2 - \Delta)^n} &= \frac{(-1)^{n-1} i}{(4\pi)^{\frac{d}{2}}} \frac{d}{2} \frac{\Gamma(n - \frac{d}{2} - 1)}{\Gamma(n)} \left(\frac{1}{\Delta}\right)^{n - \frac{d}{2} - 1}, \\ \int \frac{d^d \ell}{(2\pi)^d} \frac{\ell^\mu \ell^\nu}{(\ell^2 - \Delta)^n} &= \frac{(-1)^{n-1} i}{(4\pi)^{\frac{d}{2}}} \frac{g^{\mu\nu}}{2} \frac{\Gamma(n - \frac{d}{2} - 1)}{\Gamma(n)} \left(\frac{1}{\Delta}\right)^{n - \frac{d}{2} - 1}, \\ \int \frac{d^d \ell}{(2\pi)^d} \frac{(\ell^2)^2}{(\ell^2 - \Delta)^n} &= \frac{(-1)^n i}{(4\pi)^{\frac{d}{2}}} \frac{d(d+2)}{4} \frac{\Gamma(n - \frac{d}{2} - 1)}{\Gamma(n)} \left(\frac{1}{\Delta}\right)^{n - \frac{d}{2} - 2}, \\ \int \frac{d^d \ell}{(2\pi)^d} \frac{\ell^\mu \ell^\nu \ell^\rho \ell^\sigma}{(\ell^2 - \Delta)^n} &= \frac{(-1)^n i}{(4\pi)^{\frac{d}{2}}} \frac{\Gamma(n - \frac{d}{2} - 2)}{\Gamma(n)} \left(\frac{1}{\Delta}\right)^{n - \frac{d}{2} - 2} \\ &\quad \times \frac{1}{4} (g^{\mu\nu} g^{\rho\sigma} + g^{\mu\rho} g^{\nu\sigma} + g^{\mu\sigma} g^{\nu\rho}). \end{aligned} \quad (\text{D.3})$$

If the integral converges, one can set $d = 4$ from the start, if not the behavior near $d = 4$ can be extracted by expanding

$$\left(\frac{1}{\Delta}\right)^{2-\frac{d}{2}} = 1 - \left(2 - \frac{d}{2}\right)\log\Delta + \dots . \quad (\text{D.4})$$

The expansion for $\Gamma(x)$ near its pole:

$$\Gamma(x) = \frac{1}{x} - \gamma + O(x) , \quad (\text{D.5})$$

near $x = 0$ and the γ is the Euler-Mascheroni constant, $\gamma \approx 0.5772$. And also the following equation often appears in calculations:

$$\frac{\Gamma(2 - \frac{d}{2})}{(4\pi)^{\frac{d}{2}}} \left(\frac{1}{\Delta}\right)^{2-\frac{d}{2}} = \frac{2}{\epsilon} - (\log\Delta + \gamma - \log(4\pi)) + O(\epsilon) , \quad (\text{D.6})$$

with $\epsilon = 4 - d$.

The d-dimensional Fourier transformation is given as

$$\int d^d x \frac{e^{ip \cdot x}}{(-x^2)^n} = -i\pi^2 \frac{\Gamma(\frac{d}{2} - n)}{\Gamma(n)} 2^{d-2n} \left(-\frac{1}{p^2}\right)^{\frac{d}{2}-n} , \quad (\text{D.7})$$

and the inverse Fourier transformation will give

$$\frac{1}{(x^2)^n} = \int \frac{d^d p}{(2\pi)^d} e^{-ip \cdot x} i(-1)^{n+1} 2^{d-2n} \pi^{\frac{d}{2}} \frac{\Gamma(\frac{d}{2} - n)}{\Gamma(n)} \left(-\frac{1}{p^2}\right)^{\frac{d}{2}-n} \quad (\text{D.8})$$

APPENDIX E

THE FULL PROPAGATOR FOR THE LIGHT QUARK

$$\begin{aligned}
iS_q^{\alpha\beta}(x) &\equiv \langle 0|T[q_a^\alpha(x)\bar{q}_b^\beta(0)]|0\rangle \quad (a, b: \text{color indices}, \alpha, \beta: \text{spinor indices}) \\
&= \frac{i}{2\pi^2} \frac{1}{(x^2)^2} \cdot \delta_{ab} \cdot \not{x}^{\alpha\beta} - \frac{1}{12} \cdot \delta_{ab} \delta^{\alpha\beta} \langle \bar{q}q \rangle \\
&\quad - \frac{1}{192} x^2 \cdot \delta_{ab} \delta^{\alpha\beta} g \langle \bar{q}\sigma \cdot Gq \rangle \\
&\quad + \left(-\frac{i}{32\pi^2} \right) \frac{1}{x^2} \cdot g_s G_{\mu\nu}^A t_{ab}^A (\not{x}\sigma^{\mu\nu} + \sigma^{\mu\nu} \not{x})^{\alpha\beta} \\
&\quad + \left(-\frac{\pi^2}{3^3 2^7} \right) x^4 \cdot \delta_{ab} \delta^{\alpha\beta} \langle \bar{q}q \rangle \left\langle \frac{\alpha_s}{\pi} G^2 \right\rangle \\
&\quad + \left(-\frac{1}{4\pi^2} \right) \frac{1}{x^2} \cdot \delta_{ab} \delta^{\alpha\beta} \cdot m_q + \frac{i}{48} \cdot \delta_{ab} \cdot m_q \langle \bar{q}q \rangle \not{x}^{\alpha\beta} \\
&\quad + \frac{i}{3^2 2^7} x^2 \cdot \delta_{ab} \cdot m_q g \langle \bar{q}\sigma \cdot Gq \rangle \not{x}^{\alpha\beta} \\
&\quad + \left(-\frac{1}{32\pi^2} \right) \left[\ln\left(-\frac{x^2 \Lambda^2}{4}\right) + 2\gamma_{EM} \right] \cdot m_q \cdot g_s G_{\mu\nu}^A t_{ab}^A (\sigma^{\mu\nu})^{\alpha\beta} \\
&\quad + \frac{i}{8\pi^2} \frac{1}{x^2} \cdot \delta_{ab} \cdot m_q^2 \cdot \not{x}^{\alpha\beta} + \frac{1}{96} x^2 \cdot \delta_{ab} \delta^{\alpha\beta} \cdot m_q^2 \langle \bar{q}q \rangle \\
&\quad + \frac{i}{2^7 \pi^2} \left[\ln\left(-\frac{x^2 \Lambda^2}{4}\right) + 2\gamma_{EM} \right] m_q^2 \cdot g_s G_{\mu\nu}^A t_{ab}^A (\not{x}\sigma^{\mu\nu} + \sigma^{\mu\nu} \not{x})^{\alpha\beta} \\
&\quad + \frac{1}{3^2 2^8} x^4 \cdot \delta_{ab} \delta^{\alpha\beta} \cdot m_q^2 g \langle \bar{q}\sigma \cdot Gq \rangle \\
&\quad - \frac{i}{3^5 2^5} x^2 \cdot \delta_{ab} \cdot g_s^2 \langle \bar{q}q \rangle^2 \not{x}^{\alpha\beta} - \frac{1}{3^5 2^7} x^4 \cdot \delta_{ab} \delta^{\alpha\beta} \cdot m_q g_s^2 \langle \bar{q}q \rangle^2 \quad (E.1)
\end{aligned}$$

APPENDIX F

THE BOREL TRANSFORMATION

The definition of the Borel transformation is

$$\hat{L}^{-1} \equiv \lim_{Q^2, n \rightarrow \infty} \frac{(Q^2)^n}{(n-1)!} \left(\frac{-d}{dQ^2} \right)^n, \quad M^2 \equiv \frac{Q^2}{n} (= \text{finite}) . \quad (\text{F.1})$$

The transformation of typical functions in QCD sum rules are given as,

$$e^{(-zQ^2)} \rightarrow \delta(zM^2 - 1) , \quad (\text{F.2})$$

$$(Q^2)^n \ln Q^2 \rightarrow (-1)^{n+1} n! (M^2)^n , \quad (\text{F.3})$$

$$\alpha_s(Q^2) (Q^2)^n \ln Q^2 \rightarrow (-1)^{n+1} n! \alpha_s(M^2) (M^2)^n + \dots , \quad (\text{F.4})$$

$$\frac{1}{(Q^2)^n} \rightarrow \frac{1}{(n-1)! (M^2)^n} , \quad (\text{F.5})$$

$$\begin{aligned} \frac{\alpha_s(Q^2)}{(Q^2)^n} &\rightarrow \frac{1}{(n-1)! (M^2)^n} \frac{4\pi}{b \ln(M^2/\Lambda^2)} \left[1 + O\left(\frac{1}{\ln(M^2/\Lambda^2)} \right) \right] \\ &\rightarrow \frac{\alpha_s(M^2)}{(n-1)! (M^2)^n} + \dots , \end{aligned} \quad (\text{F.6})$$

$$\frac{1}{(Q^2 + m^2)^n} \rightarrow \frac{1}{\Gamma(n) (M^2)^n} e^{\frac{-m^2}{M^2}} , \quad (\text{F.7})$$

where the ... denotes higher order α_s corrections.

Practically, the following explicit table is useful:

$$\begin{aligned}
q^4 \ln(-q^2) &= Q^4 \ln Q^2 &\rightarrow & -2M^4 , \\
q^2 \ln(-q^2) &= -Q^2 \ln Q^2 &\rightarrow & -M^2 , \\
\ln(-q^2) &= \ln Q^2 &\rightarrow & -1 , \\
\frac{1}{q^2} &= -\frac{1}{Q^2} &\rightarrow & -\frac{1}{M^2} , \\
\frac{1}{q^4} &= \frac{1}{Q^4} &\rightarrow & \frac{1}{M^4} , \\
\frac{1}{q^6} &= -\frac{1}{Q^6} &\rightarrow & -\frac{1}{2M^6} .
\end{aligned} \tag{F.8}$$

CURRICULUM VITAE

PERSONAL INFORMATION

Surname, Name: Saraç , Yasemin

Nationality: Turkish (TC)

Date and Place of Birth: 9 October 1976, Kırıkkale

Phone: +90 312 210 43 28

email: ysarac@metu.edu.tr

EDUCATION:

High School: Anadolu Öğretmen Lisesi, Afyon, 1995

B.S.: METU, The Faculty of Education, Department of The Science Education,
Physics Education Programme, June 2000.

M.Sc: METU, The Graduate School of Natural and Applied Sciences, Physics,
August 2001.

PUBLICATIONS

1. A. Gokalp, Y. Sarac, O. Yilmaz, Scalar a_0 -meson Contribution to Radiative $\omega \rightarrow \pi^0 \eta \gamma$ and $\rho^0 \rightarrow \pi^0 \eta \gamma$ Decays, Eur. Phys. Jour. C 22, 327(2001) .
2. A. Gokalp, Y. Sarac, O. Yilmaz, The Coupling Constant $g_{a_0 \pi \eta}$ as Derived From Light-Cone QCD Sum Rules, Mod. Phys. Lett. A 19, 3011(2004) .

3. A. Gokalp, Y. Sarac , O. Yilmaz, An Analysis of $f_0 - \sigma$ Mixing in Light Cone QCD Sum Rules, Phys. Lett. B609, 291 (2005) .
4. Y. Sarac, H. Kim, S. H. Lee, QCD Sum Rules for the Anti-charmed Pentaquark, Phys. Rev. D 73, 014009 (2006) .